UNIVERSITÀ POLITECNICA DELLE MARCHE

FACOLTÀ DI INGEGNERIA

Corso di Laurea Magistrale in Ingegneria

Informatica e Automazione

Design and implementation of optical sensor for wastewater analysis

Progettazione e realizzazione di un sensore ottico per l'analisi di acque reflue

Relatore: David Scaradozzi

Correlatore: Domenico Santoro

Tesi di Laurea di:

Giorgio Antonini

A. A. 2021 / 2022

Engineering Department

Master's Degree Course in Computer and Automation Engineering

Ai miei genitori Enrico e Maria e
A mia nonna Lia

Engineering Department

Master's Degree Course in Computer and Automation Engineering

Index

List of Figures

Abstract

Il lavoro svolto e illustrato in questa tesi è stato realizzato in collaborazione tra l'Università Politecnica delle Marche e la University of Western Ontario, con l'obiettivo di analizzare e confermare l'idea proposta dal professore di ricerca aggiunto Domenico Santoro nell'ambito del monitoraggio delle acque reflue.

L'obiettivo principale del progetto è stato quello di valutare un metodo non convenzionale per testare la qualità dell'acqua, in particolare delle acque reflue. La creazione di un nuovo sensore, a basso costo, che permetta di valutare le anomalie e le variazioni delle caratteristiche qualitative dell'acqua basandosi sull'utilizzo di una telecamera industriale USB e di una sorgente luminosa costituita da diversi LED con varie lunghezze d'onda.

La tesi risulta strutturata in diversi capitoli che affrontano lo stato dell'arte, i materiali e metodi adottati, i risultati ottenuti dai vari test effettuati con la strumentazione con i dovuti confronti e analisi e infine i possibili sviluppi futuri dell'idea e del lavoro realizzato.

Nel capitolo che va a descrivere lo stato dell'arte si introduce l'oggetto delle analisi: le acque reflue. Queste vengono descritte per la loro composizione che le va a differenziare in diverse tipologie e diversi trattamenti necessari prima di poter essere immesse nuovamente nell'ambiente senza causare danni. Successivamente vengono introdotti diversi sensori che vengono utilizzati nel settore e in particolar modo si approfondisce la tematica di sensori legati alla torbidità delle acque; viene fatta una sintesi dei diversi sensori attualmente utilizzati con un paragone tra i metodi esistenti e quello realizzato per questo lavoro, andando a sottolineare le problematiche attuali e i possibili vantaggi del metodo introdotto. Infine, viene fatta una descrizione introduttiva sui sensori utilizzati dalla camera e sulle differenti proprietà della luce che risultano essere d'interesse in questo particolare ambito applicativo.

Nel capitolo, Materiali e Metodi viene fatta una panoramica sul sistema realizzato a partire dalla modellazione 3D alla realizzazione del sistema di alimentazione e raffreddamento. Nel dettaglio si vanno a mostrare la camera e la lente scelta con le loro caratteristiche tecniche, insieme alle luci LED utilizzate con le diverse lunghezze d'onda e proprietà. Affianco a ciò si va a descrivere il procedimento e i metodi utilizzati per calibrare il modello: la camera, con i diversi parametri, LED con l'intensità luminosa il tutto attraverso diversi test volti a determinare parametri che facessero in modo di non saturare i valori dei pixel della camera.

I risultati ottenuti dai diversi test sono riportati nel capitolo 4. In particolare, si fa riferimento a dei test che hanno avuto lo scopo di validare il modello andando a confrontare i risultati ottenuti da quest'ultimo con due strumenti dell'azienda *Hach:* un turbidimetro e uno spettrometro. I test sono stati realizzati su campioni di refluo secondario presi ogni ora per 4 giorni consecutivi dall'impianto di depurazione di Hilderton. Dunque, al termine del capitolo vengono fatte le dovute considerazioni sui risultati ottenuti sul confronto dei dati raccolti.

In ultima analisi vengono proposti diversi sviluppi a cui questo sistema può andare incontro e delle diverse applicazioni alle quali, un sistema low cost come quello realizzato, può risultare utile e fornire un vantaggio sull'attuale stato dell'arte.

Chapter 1: Introduction

The work performed and showed in this thesis has been realized in collaboration between the Università Politecnica delle Marche and the University of Western Ontario, with the aim of analyzing and confirm the idea proposed by the *Adjunct Research Professor* Domenico Santoro in the wastewater monitoring framework.

The project main goal has been to evaluate a non-conventional method to test the quality of water, in particular of wastewaters. The creation of new, low cost, sensor has to evaluate the anomalies and the variation in the qualitative characteristics of the water based on the use a USB-industrial camera and a light source made by different LEDs with several wavelengths.

The thesis is structured in several chapters that deal with the state of the art, the materials and methods adopted, the results obtained from the various tests carried out with the instrumentation with the necessary comparisons and analyzes and finally the possible future developments of the idea and of the work carried out

Hence, in the following chapters the core of the work is exposed, trying to briefly describe the huge framework in which this system is going fit, highlighting how the results have been obtained and what they could mean.

Chapter 2: Problematic and State-Of-The-Art

In this historical moment, technology has allowed the achievement of objectives and results not even imaginable until a few decades ago; the reduction of costs, the miniaturization of electronics are just the tip of the iceberg. In this chapter, in a synthetic way, it has been tried to report the current state of the art as regards the technologies adopted and the problems faced in the sector in which the project is inserted.

2.1 Wastewaters and their Proprieties

Water has always been not a resource but the fundamental resource for man to survive, develop and prosper. In recent decades, as demonstrated by data and various studies in this regard (Chunyang *et al.* 2021; Flannery *et al.* 2021), population growth and climate change are making water more and more precious due to ever smaller quantities available. For this reason and for others, related not only to re-use but also to pollution and the safety of people and the environment, wastewaters' treatments have become a sector where investments at community and industrial level have increased significantly. Wastewaters are all waters that have been modified in their composition by human activity, be it domestic, agricultural or industrial, through organic and inorganic contaminants dangerous to public health and the natural environment. Precisely for these reasons it is not possible to reintroduce the latter into the environment as the balance of the ecosystem, which is the final delivery, would be compromised, failing to manage such a quantity of polluting substances. As mentioned above, the origin of the waters is various, as is their composition and therefore their subsequent treatment, which will be described in the following *section 2.2*.

- *Domestic wastewater*: comes from urban areas and services, mainly deriving from human metabolism and domestic activities, above all: cellulose, lipids, protein substances, carbohydrates, urea, and urea acid. Nowadays, however, it must be taken into consideration the fact that dozens of chemicals from soaps, crams etc. are added to these substances which without realizing they have become part of daily life, and which end up in the drains. In fact, this category includes not only houses but also hotels, public and private offices, local retail and wholesale shops and many other businesses which,

as you can well imagine, have waste that does not always fall within the scope of deriving from the metabolism and for that reason have a more arduous management.

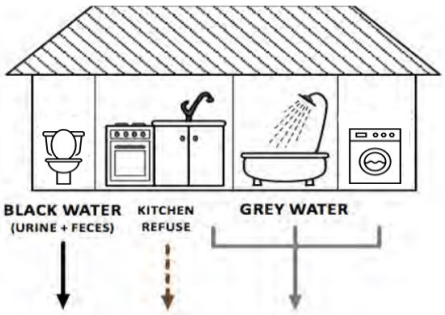

Figure 1: Domestic Wastewater Scheme

- *Industrial wastewater*: for industrial wastewater it has been considered those coming from buildings and installations in which goods production activities take place, (also subjected to preventive purification treatment), qualitatively different from domestic ones; the characteristics of this waste are highly variable based on the activities carried out in the production plant and are generally divided into dangerous and non-dangerous for the environment.

- *Urban wastewater*: resulting from a mix of both domestic and industrial wastewater, and/or runoff, i.e. runoff, street washing water, etc. which is conveyed into sewage networks; in particular the so-called runoff waters contain various micro pollutants such as hydrocarbons, pesticides, detergents and even rubber debris.

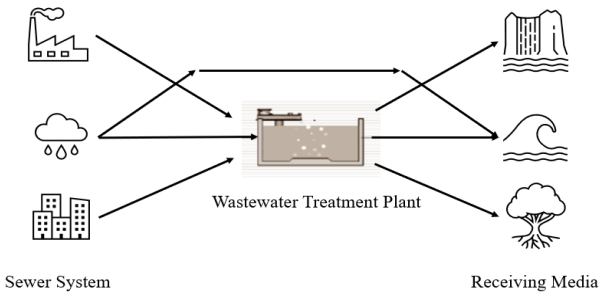

Figure 2: Urban Wastewater Scheme

The substances that are present in the liquid are different and categorized not only by chemical composition and origin but also by the size of the particles inside it. In fact, there

are floating substances such as oils, fats, foams, and compounds in general which are lighter than water and float in it. Then, there are the suspended substances which are insoluble in water but with a density greater or almost equal to water and are kept in suspension due to the turbulence present. These substances are divided into sedimentable and non-sedimentable. Another type of substances are colloidal ones, they have particles of such dimensions that they cannot be separated from the water through a mechanical treatment (10^{-9} - 10^{-7} m). Finally, there are the so-called dissolved substances which are homogeneously dispersed at the molecular or ionic level of the water and in addition to all this, biological materials representing the various animal and vegetable organisms present in the wastewater must also be considered.

For each of the types described above, it is possible to carry out a further separation into:

- non-volatile solids (or fixed residue): represents the residue obtained after incineration in a muffle furnace at a temperature of 600°C
- volatile solids: this is the definition of solids which gasify at 600°C and therefore remain as ashes.

To identify the different substances in the wastewater and characterize it, various physical, chemical, and biological parameters are taken into consideration which are characteristic of both industrial and civil wastewater, while others are typical only of industrial wastewater.

Parameters Considered	
Physical Parameters	○ Temperature ○ Electrical Conductivity ○ Solids ○ Color ○ Smell
Chemical Parameters	○ pH ○ Alkalinity ○ Inquiry for: Chemical Oxygen Demand (COD), Biochemical Oxygen Demand (BOD), Total Oxygen Demand (TOD) ○ Total Organic Carbon (TOC) ○ Nitrogen: Organic, Nitrites, Nitrates ○ Phosphorus: Orthophosphates, Polyphosphates, Organic ○ Oils and Fats ○ Mineral Oils ○ Surfactants ○ Toxic Substances ○ Dissolved Oxygen
Biological Parameters	○ Total Coliforms ○ Fecal Coliforms ○ Fecal Streptococci ○ Escherichia Coli ○ Salmonella

Table 1: Wastewater Parameters Considered

The work carried out aims to evaluate possible differences in the wastewater, thus looking for variations detected by the camera, signs of a possible anomaly inside the treatment plant: a different composition, such as to modify the turbidity of the sample and symptom of a system that needs a more in-depth analysis to explain the causes.

2.1.1 Wastewaters' Current Treatments

As said previously, wastewaters refer to used waters coming from houses, businesses, industries, and institutions that drain into sewers. In addition to those, sometimes they are also combined with raining water, melting snow from streets or rooftops, parking lots and roads. Those types of wastewaters before they could be released in the environment must be treated containing organic wastes, pathogens, microorganisms, industrial chemicals very risky for the human and environmental health.

In particularly, in Canada, there are two federal acts: the Fisheries Act and the Canadian Environmental Protection Act. Those laws develop regulations on releasing of harmful and toxic substances into the environment. There are various levels of wastewater treatment; there are primary, secondary, and tertiary levels of treatments. As showed in the *figure 3*, most wastewater is treated through secondary treatment, the data shown made available by the Canadian authorities themselves.

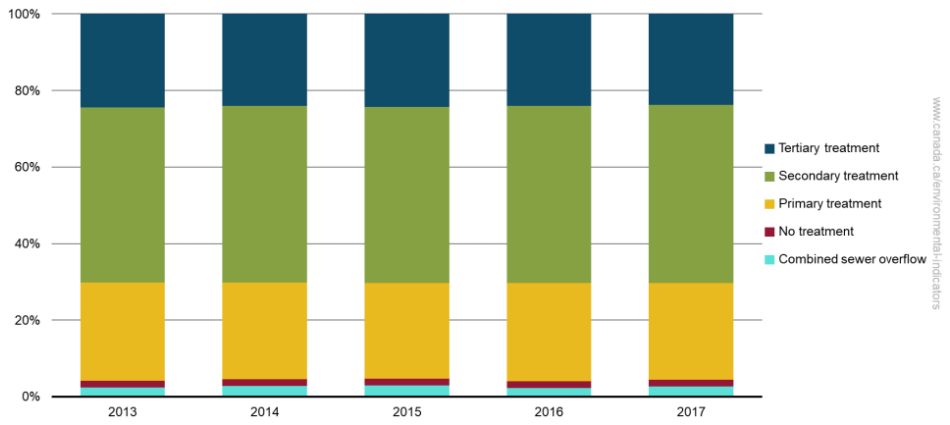

Figure 3: Proportion of municipal wastewater volume discharged by treatment category, Canada, 2013 to 2017

The primary treatment is used to remove the majority of solids throughout screens and settling tanks. This step is crucial, in fact 35 % of the pollutants are solids and must be removed. Usually, the used screens have openings of 10 mm, which are enough to block the large materials and separate it from the wastewater. This first treatment removes up to 50 % of Biological Oxygen Demand (BOD) and almost the 90 % of suspended solids. In the *figure*

4, the primary treatment is schematized, but as mentioned, even if it is efficient and mandatory it is not enough to ensure that all dangerous wastes have been removed.

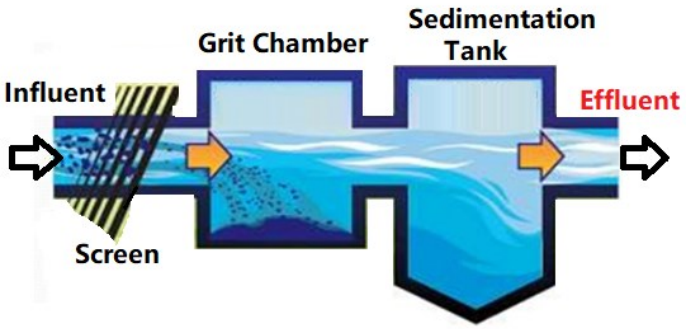

Figure 4:Primary Treatment Scheme

The secondary treatment uses bacteria to digest the pollutants remained in the wastewater. In order to have this process correctly done and in a faster way the settling tanks are 'drugged' with bacteria and oxygen; the oxygen helps those bacteria to digest the pollutants with the result of a faster process. This process, that can take hours, remove up to 95 % of pollutants and in particularly around 85 – 90 % of BOD and up to 99 % of coliform bacteria.

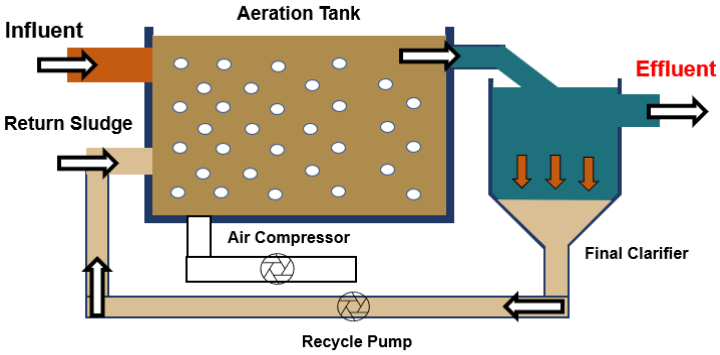

Figure 5: Secondary Treatment Scheme

The tertiary treatment is the most advanced and its aim is to eliminate dissolved substances like metals, organic chemicals, and nutrients such as phosphorus and nitrogen. There are several treatment processes used during the third step and they are physical, chemical and biological.

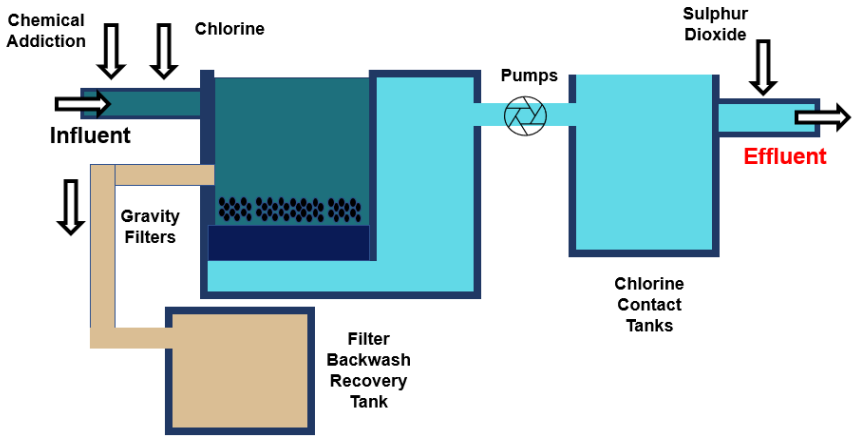

Figure 6: Tertiary Treatment Scheme

Obviously, what is shown in the diagrams above are, indeed, diagrams and are meant to summarize what the real treatments are. In the table below, adapted from the one used in the Canadian government document (Environment and climate change Canada 2020) some other details on the specific steps are described.

Treatment Category	Definition
Primary Treatment	At least one of the following processes is applied: • Chemical flocculation • Primary sedimentation/clarification • Skimming
Secondary Treatment	At least one of the following processes is applied: • Activated sludge system (with or without extended aeration) • Activated sludge system (with or without pure oxygen) • Lagoon systems (one or combination of aerated, aerobic, anaerobic, facultative, non-aerated, non-aerated filtered) • Oxidation ditch • Rotating biological contactor • Storage ponds (polishing ponds) • Sequencing batch reactor • Trickling filter • Integrated systems that combine the above technologies • Chemical precipitation for phosphorus
Tertiary Treatment	At least one of the following processes is applied: • Biofiltration • Biological ammonia removal – nitrification only • Biological ammonia removal – nitrification and denitrification • Biological ammonia removal (nitrogen and phosphorus) • Biological phosphorus removal • Filtration • Peat filter • Integrated systems that combine the above technologies with secondary treatments technologies or some systems that only apply tertiary methods

Table 2: Different Processes for Wastewater

What is common between Italy, Canada, and off course all other countries are the difficulties in managing wastewater's treatments in rural communities. In fact, the physical geography and the population density have a huge influence and became factors that cannot be ignored; referring to Canadian situation several communities have inadequate methods of treating wastewater, some of them discharge untreated water and others leading the way with innovative methods of treating and water conservation measures.

The camera sensor designed according to this project worked with wastewaters coming from a secondary treatment sampled in the Greenway and Ilderton facilities.

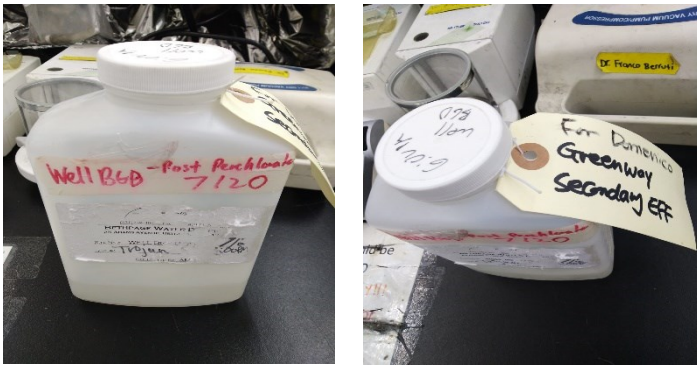

Figure 7: Secondary Effluent Sample

Those wastewater treatment plants do not have a tertiary treatment, but they implement filters downstream of the secondary treatment giving the chance of testing the system with various samples with different amount of suspend particles in the solution; this have given the chance of analyze how much the particles' presence have an impact on the results occurred.

2.2 Currently Used Sensors

Nowadays the number of sensors arranged within plants to keep everything under control and check the wastewater's quality, reaches into the hundreds depending on the size of the plant itself. The type of sensors also depends on the level of treatment carried out within the treatment plant, these generally measure key characteristics of the liquid such as conductivity, pH, salinity, temperature, dissolved oxygen, chlorine residual and finally turbidity, which is what the system created should measure, as it is explained more deeply in *section 2.2.1*.

Conductivity sensors measure the total ionic concentration in aqueous solutions, and they are fundamental to gain information such as dissolved compounds; they are largely used in wastewater facilities, clean in place control and measurement of concentration levels in solutions.

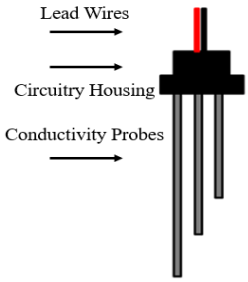

Figure 8: Conductivity Sensor Scheme

Sensors measuring water's pH are important too; they indicate how acid or basic the solution is, and they usually have a measuring electrode that works with thresholds that cannot be exceeded.

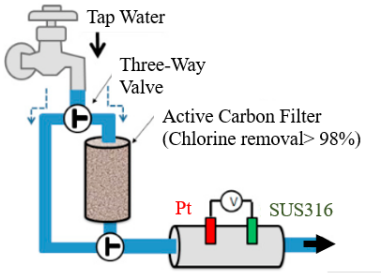

Figure 9: pH Sensor Scheme

Another commonly used are the ones that measure the Oxygen-Reduction Potential (ORP) of a solution, providing insight into the level of oxidation/reduction reactions occurring in the wastewater.

Chlorine residual sensors measure the chlorine residual in drinking water treatment, which is its primary application, but they are used in the reclaimed wastewater; in fact, chlorine is the most common disinfectant used because of its efficiency and costs.

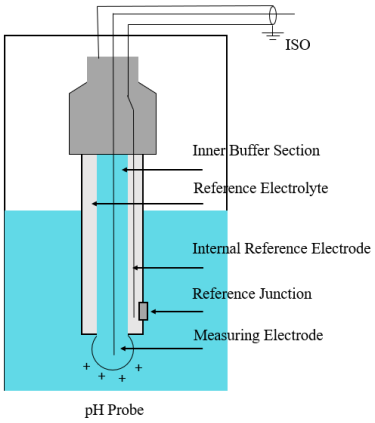

Figure 10: Chlorine Sensor Scheme

Total Organic Carbon (TOC) has two different measurement devices available: one is a TOC analyzer, and the other is a TOC sensor. For obvious reasons the choice falls on use and how precise the measurement needs to be.

2.2.1 Turbidity

Turbidity sensors aim to measure suspended solids in water, so turbidimeters usually works calculating the amount of light transmitted through the water. Apart from wastewater field, this characteristic is used in other applications such as the medical (Andrea G. Mann *et al*. 2007; R.D. Morris *et al*. 1996), pharmaceutical industry as described in the article *Self Emulsifying Drug Delivery System* of 2010. Other applications are the examination of environmental dredging described by Pennekamp in *Turbidity caused by dredging; viewed in perspective*, or in marine biology to study the effects of turbidity on fishes' life and on other aquatic lives like coral reefs (Gustavo A. S. Duarte *et al.* 2020).

Hence, turbidimeters are used in several fields and they must follow different standards. Beyond the international standards dictated by the Geneva Convention (ISO 7027 Water quality Determination of turbidity 1999), there are others that differ from individual nations but with obvious similarities too. For example, at the European level many countries rely on what is imposed by the European council (The Council of European Union 1999; European Union 2014).) which specifies that the measurement of turbidity is not part of the guidelines for plant monitoring and that specifically to the guidelines for the treatment of drinking water

an error of no more than 25% of the turbidity measurement is accepted. Regarding Canada, although what was defined in Geneva in 1999 is accepted other standards are also taken into account, many of which are in common with what was established in the neighboring United States (American Public Health Association *et al*. 2012; ASTM International 2011).

Hence, directly referring to what is reported by the current Canadian government standards the treated water the target is 0.1 NTU (Nephelometric Turbidity Unit) but the actual levels of turbidity may vary with the technology used. Chemically filtration: turbidity shall be less than or equal to 0.3 NTU in at least 95% of the measurements and shall not exceed 1.0 NTU at any time.

- Slow sand earth filtration: turbidity shall be less than or equal to 1.0 NTU in at least 95% of the measurements and shall not exceed 3.0 NTU at any time.
- Membrane filtration: turbidity shall be less than or equal to 0.1 NTU in at least 99% of the measurements and shall not exceed 0.3 NTU at any time.

A variation in these values could mean a problem in the system or in the wastewater source, in any case it requires a check. So, it can be easily seen how the measurement of turbidity turns out to be a key parameter for measuring the quality of the water but also of the treatment plant itself. A variation in these values, coming from an effluent sample could mean a problem in the system or in the wastewater source, in any case it requires a check. There are several studies that connect turbidity to several key factors that measure the efficiency and health of the water treatment plant itself; for example, it has been noted how the TSS (Total Suspended Solids) is strictly related to turbidity level found in wastewaters (Bertrand-Krajewski 2004). So, increasing the TSS value con be provoked by an increase in turbidity in the effluent stream. The particle size distribution (PSD) is related to the liquid's turbidity and there are studies who tries to prove the correlation between those characteristics and other that tries to establish the inverse correlation between these properties COD (Wu *et al*. 2009; García-Mesa *et al*. 2010; Bersinger *et al*. 2015). Turbidity, in the wastewater field, do not depend only on dissolved organic matter (DOM) and suspended sediment but on the color too. The color may vary from green to brown, passing through yellow and the intermediate lighter and darker shades. Obviously, the dissolved substances, even if they are not considered as TSS they may still absorb light and cause cloudiness affecting the water's clarity indicating a poor water quality (Stedmon *et al.* 2015; Gitelson *et al.* 2008).

As mentioned before, the turbidity is not a measure directed of the water quality, in particular for drinking water quality, but it could be other impurities and can highlight some problems in the system in a faster way (Banna *et al.* 2014).

2.3 Technology Adopted

The technology used in this project differs to what is commonly used as a turbidimeter in practical applications. What is showed in *figure 11* is schematically how a turbidimeter works and is built; the turbidimeter presented in *figure 65* which has been used to make comparisons during the experiments carried out uses this exact working scheme.

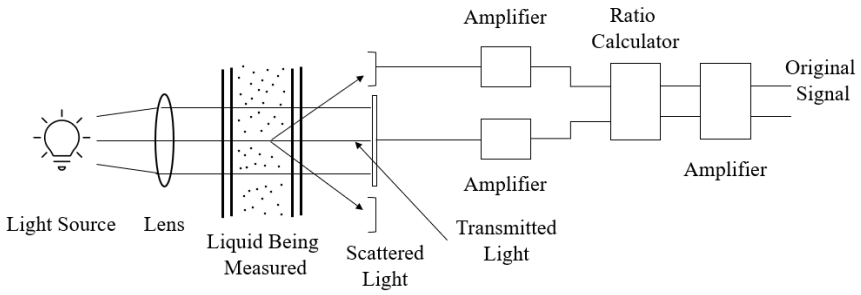

Figure 11: Turbidimeter Scheme

Right now, there are two general units of turbidity used, the first one, already mentioned, is the NTU and the second one is the FAU (Formazin Attenuation Units). The two units of measure are different for the method itself of how the measurement is acquired (Telesnicki, Goldberg 1995). On NTU instruments, such as the Hach 2100Q, the values are calculated measuring the scattered light from the sample at a 90-degree angle to the incident light; on the other hand, the FAU instruments try to measure the transmitted light through the sample at an angle of 180 degree to the incident light (this particular method is used with spectrophotometer or colorimeter). Modern turbidimeters allow to take measures in lab and directly in the plant.

The ones in-situ have the advantage of rapidity giving results right away comparing to the ones in labs that must follow longer procedures (Jouanneau *et al*. 2014). A study carried out in small scale applications demonstrated how measuring the refractive index of the effluent

stream can detect water quality problems like turbidity itself (de Graaf *et al*. 2012; Williamson *et al*. 2014). However, those type of sensors are stable and reliable only under specific conditions such as a stable organic load and particular chemical parameters; in addition to these issues, sensors are found to work immersed in water, and prolonged contact with water causes them to be inaccurate or require constant maintenance and calibration checks (Joannis *et al*. 2008). Specifically, to the wastewater's application field the prolonged submerged in turbid fluids can bring organic materials over the sensors and this create the necessity of regular cleaning and calibration. Hence, even if the current automated solutions can give some advantages and in ideal condition, cleaned and calibrated, are accurate too; most of the times they are untrustworthy after only a few days without checks causing problems in larger plants, for the high numbers of sensors deployed and in the smaller ones because the monitoring is less frequent, and they do not guarantee technicians onsite constantly.

Those problems make this kind of solution unsuitable for long term monitoring of diversified samples. A first option as an automated system has been proposed by Darragh Mullins, Derek Coburn and Louise Hannon in the article *A novel image processing-based system for turbidity measurement in domestic and industrial wastewater.* They have proposed a new way to estimate the water's turbidity using a digital camera and analyzing the images. What has been done by Mullins in 2018 has the same principles and aims what has been implemented during this work:

- Reducing the costs of professional instruments using a camera, implementing a sensor that can detect changes and anomalies without the need of a real spectrophotometer or turbidimeter.
- Removing the necessity of manual observations made by operators which, as said explained in the sections above, are widely used in the wastewater industry to get quality information (Hannon 2016).

2.3.1 Light

As mentioned in the previous section, turbidity is studied and evaluated through light and its various phenomena and properties. In fact, through the calculation of absorbance, depth of

penetration and through the analysis of phenomena such as fluorescence and scattering that much useful information about water quality can be obtained.

As is well known, light is a wave phenomenon, and it is precisely the different wavelengths of light rays that turn out to be important in defining what is called the electromagnetic spectrum of which in this context only what is defined as the visible spectrum is relevant. In truth, as also explained later, the chosen camera also allows capturing wavelengths beyond those of the visible (400 nm- 700 nm), being sensitive to UVA rays but also going so far as to capture those defined as NIR.

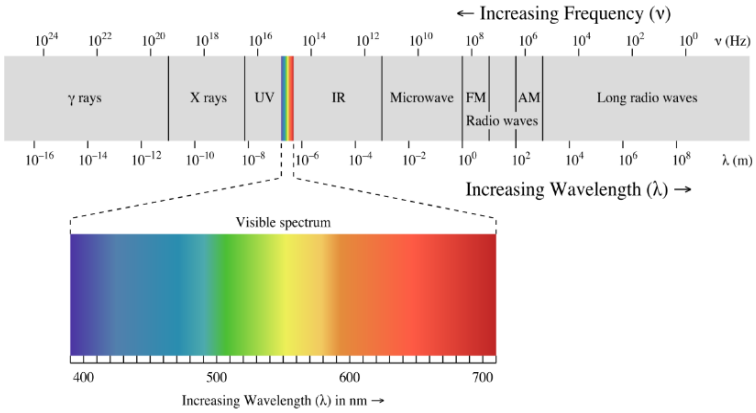

Figure 12: Electromagnetic Spectrum

Let I_0 be the intensity of a monochromatic light striking a cuvette containing a solution: part of the intensity of the incident light may be absorbed by the solution; therefore, a radiation with intensity $I \leq I_0$ will emerge from the cuvette. So, absorbance is a physical quantity that finds application in spectrophotometry.

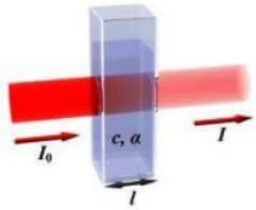

Figure 13: Absorbance Working Scheme

So, to define absorbance we must remember transmittance; this is a quantity seen as the ratio of I to I_0 and defined as $T = \frac{I}{I_0}$. Thus, absorbance can be defined as the inverse logarithm of transmittance and is dimensionless and therefore has no units of measurement

$$A = \log \frac{1}{T} = \log \frac{I_0}{I}$$

Following what is Lambert-Beer's law, absorbance can also be calculated through the following formula

$$A = \varepsilon \, l \, C \quad \text{or} \quad \frac{A}{A_0} = e^{-\varepsilon C l}$$

- A = Absorbance
- ε = molar absorption coefficient or absorptivity, the unit of which is $M^{-1}\, cm^{-1}$ (a factor that depends on the chemical species under consideration and the wavelength of the absorbed radiation and the solvent used
- l = thickness in cm of the solution crossed by the ray (optical path)
- C = concentration of the solution in mol / L

Another property of water is its ability to absorb so much of the incident light; the depth of light penetration in water is easily seen in the ocean in which light dims very rapidly as depth increases. In *figure 14*, it can be seen that this never exceeds 200 meters and most of it stops within the first ten or so meters, particularly the higher frequencies of the visible spectrum.

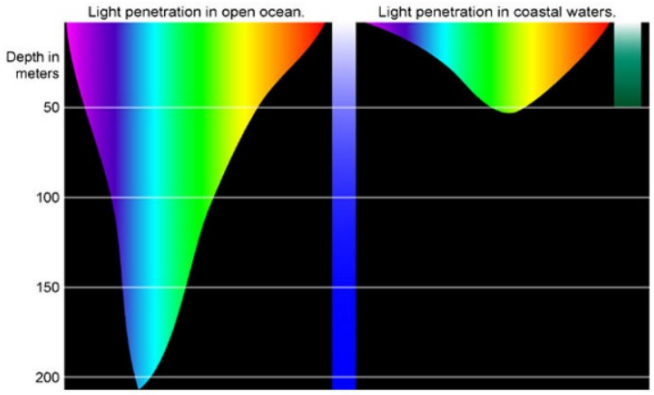

Figure 14: Light Penetration

At 10 meters depth only 16 percent of the light is still present. Wavelengths near the extremes of the visible spectrum are attenuated faster, and in general those that are able to penetrate

the most are blue and green. Note also, how there is a noticeable difference between open sea and coastal areas due to a difference in water composition and proximity to the seabed. Precisely in this regard in the field of sewage and that therefore take on not only colors but also quite different compositions there are even more important results, having depths reduced by several orders of magnitude. In this regard, in the article *Influence of Water Depth on Microalgal Production, Biomass Harvest, and Energy Consumption in High-Rate Algal Pond Using Municipal Wastewater* by Byung-Hyuk Kim it is shown how, when faced with wastewater the depth of penetration becomes on the order of tens of centimeters, making the choice of the thickness of the water to be interrogated of paramount importance.

Another property that turns out to be important is fluorescence. It is a characteristic of some substances to re-emit at longer wavelengths the electromagnetic radiation they receive. This occurs with radiation in the ultraviolet that is re-emitted in the visible, and it is a process that occurs in all materials that contain fluorescent pigments, and there are a variety of applications in the environmental, medical, but also in water treatment. In this area there are studies, for example, on how DOMs interact at the absorbance and fluorescence level (Hambly *et al*. 2015; Logue *et al*. 2016). Another notable one is the European *FLUORO-BOOST* project aims to improve the energy efficiency of wastewater treatment through spectroscopy and fluorescence.

The phenomenon of scattering refers to all those radiation-matter interactions in which waves or particles are deflected due to collision with other particles or waves. Most of the time, deflection occurs randomly, and for this very reason it is distinguished from phenomena such as reflection and refraction that change trajectory in a determined manner. Depending on the contexts, there are different types of scattering that depend, as in the case examined with the realized system, on the size of the particles. In fact, the realized system was tested to demonstrate what is called Mie scattering as shown by the results in *section 4.3.1.* While Reyleigh scattering occurs with small particles (about 1/10 of the interacting wavelength), with larger particles, such as in the case of impurities inside wastewater, we speak of Mie scattering leading to more forward scattered radiation. So, if the particles are greater than 1/10 of the incident wavelength, the radiation is no longer isotropic but is more forward scattered. Schematically, the phenomenon is shown in *Figure 15.*

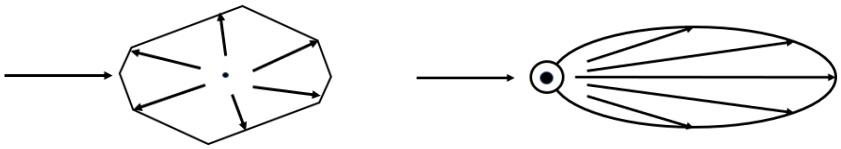

Figure 15: Reyleigh Scattering and Mie Scattering

2.3.2 Camera

In today's context, the choice of using cameras for analysis through images is becoming increasingly common because their performance and cost have definitely improved over many other technologies. Another example can be the study carried out by Tomperi *et al.* founding an optical way to monitor effluent and using it to predict suspended solids measurements in wastewater facilities.

A camera can be compared to a human eye, on one side we have the lens that allows us to focus on the other side we have the lens that is adjusted according to the distance to get a sharp image; in the eye we have the pupil that defines how much light to let in while in the corresponding we have the aperture of the camera. A key part of vision is the retina, which, located at the back, has a series of photosensitive cells, cones and rods; these photoreceptors allow for color vision and that adapts to changing light intensity in dark environments.

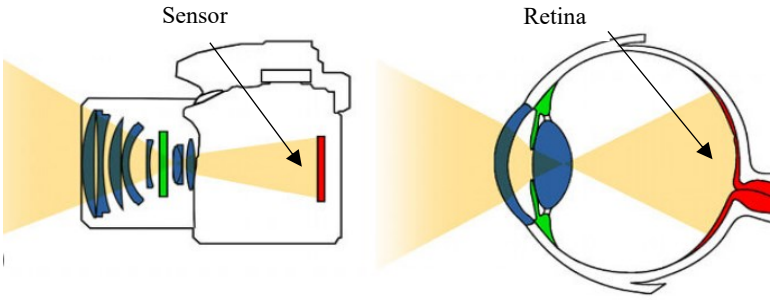

Figure 16: Camera - Eye Comparison

The mechanical equivalent is the camera sensor, which is nothing more than a silicon rectangle that serves to convert light into electrons, obtaining digital information. This process takes place thanks to the presence of photodiodes called pixels (about 80 µm) that excited by the different wavelengths impinging on them generate a potential difference proportional to the number of incident photons and therefore to the same intensity as the incident light. So, in digital cameras the sensor represents what used to be the film that was impressed during the shooting process.

The sensors all turn out to be grayscale and only then are they rendered in color through the application of a filter, the most common being the *Bayer filter*, which allows the otherwise black-and-white image to be colored.

Hence, the choice of a camera such as the one described in *Section 3.2* follows what D. Mullins also did. In fact, one of the characteristics of the camera is that it is a monochrome camera which means it doesn't work with the three channels RGB but only on a grayscale. This choice comes from the sensors itself and the characteristics of how a monochrome sensor is built differently to a color sensor. As mentioned before, all the sensors are basically monochromatic and to obtain the different colors filters are placed above all the sensor arrays; the most used is the *Bayer Filter;* this filter follows a regular path of 50 % green pixel, 25 % of red pixel and 25% blue arranged as in the *figure 17*.

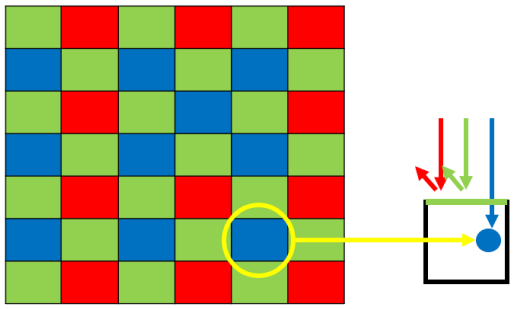

Figure 17: Bayer Filter Description

For example, in a blue pixel only incoming rays with wavelength around 470 nm can pass through the filter layer and can be absorbed by the sensor, the other wavelengths are rejected. Moreover, the second step is for reconstructing the color information on all the pixels with an operation called demosaicing or debayering. This operation goes computing the values

by averaging the nearest pixels values and to obtain a more accurate result it needs a larger mask for averaging with a consequence of a heavier and slower algorithm.

So, the light output of a color sensor cannot be compared with a monochromatic one and, as showed in the figures the monochromatic can capture in a better way the sharpness and the details thanks to a sensor that makes all the color lights through the photosites. In this project the color information was not the core, the aim was to have a clear image, with a high resolution and a minimum noise. These are the reasons above the camera that has been chosen as monochromatic over a color one.

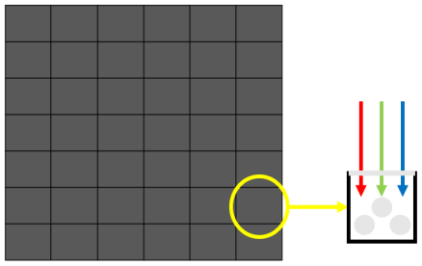

Figure 18: Monochromatic Sensor

In contrast in how it described in the article *Image processing-based turbidity measurements for wastewater monitoring* the camera has been placed facing directly the light sources giving the chance of studying differences between the samples looking directly at the LEDs lights and studying other phenomena like the scattering described in the previous section.

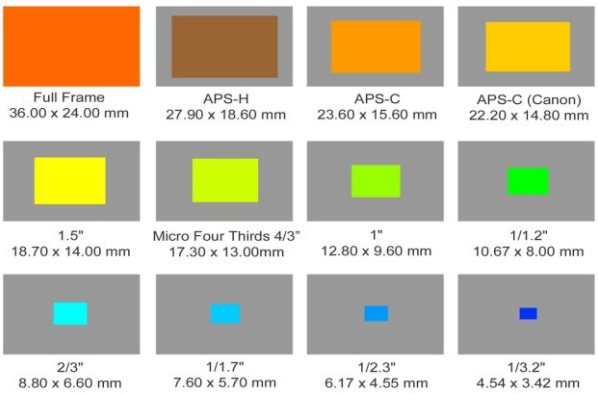

Figure 19: Sensor's Sizes

As is shown in *figure 19* the dimensions of the sensors are different and so are the acronyms that define them. First, they are measured in inches, the size is seen as the diameter of the

circle in which the rectangle (sensor) can be inscribed. Obviously, the size of the sensor has great relevance by giving the possibility of capturing more information, in fact,

Larger photodiodes can store more light than a smaller one and for this reason the images will exhibit less noise and a wider dynamic range rendering well even in high and low light situations. To remedy this, smaller photodiodes can be used, but they result in increased 'noise' by needing amplification to get a clearer image (ISO).

The size of the photodiodes is variable and should be greater than the wavelength of light that the human eye can perceive (0.4 to 0.75 μm); generally, for compact cameras the measurements are between 2 and 3 μm.

The chosen camera, *Alvium 1800U 2050*, has a type 1 (1 inch) sensor with a pixel size of 2.4 μm and is CMOS type. The CMOS (Complementary Metal Oxide Semiconductor) type sensor turns out to be more elaborate but consumes less because it converts the charges of each element independently as compared to the other family of sensors called CCD (Charge-Coupled Device), which instead uses a single amplifier at the output. Thus, the CMOS structure has advantages in terms of simplification of components resulting in lower cost and at the same time less overheating of the sensor itself making it suitable for more long-term uses.

Chapter 3: Materials & Methods

To carry out the experiments, understand if the idea was valid and verify the hypotheses underlying the project, there was a long initial process of elaborating which materials and methods had to be adopted. The path that led to the choice and creation of the first prototype was made of analysis but of trial-and-error method too. In the following pages the choices will be analyzed regarding the materials used and the experimental method adopted for instrument calibration and data acquisition

3.1 Camera-LEDs Model

The system was created with the help of a third company, outside the Western University campus or UNIVPM participation. The reliance on a specialized company has been made mandatory by the high precision required. The creation of the model was preceded by a series of steps: planning, design and finally construction. In the following pages the structure will be showed and explained.

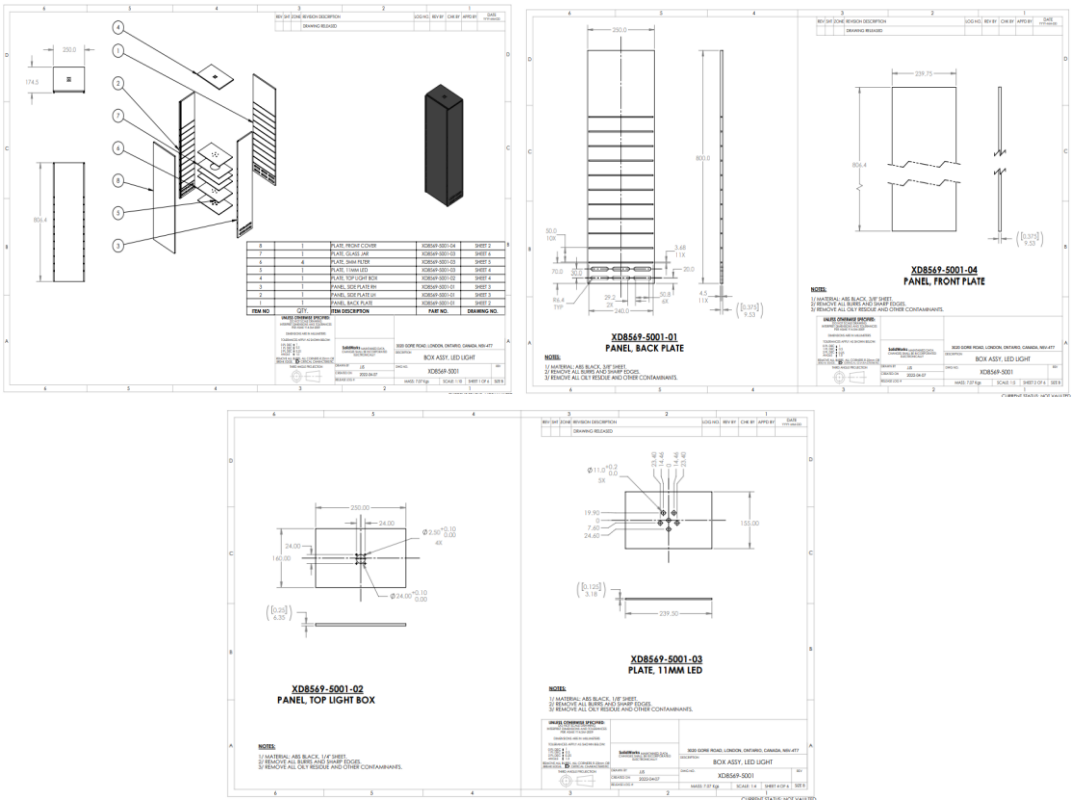

Figure 20: SolidWorks Model Drawings

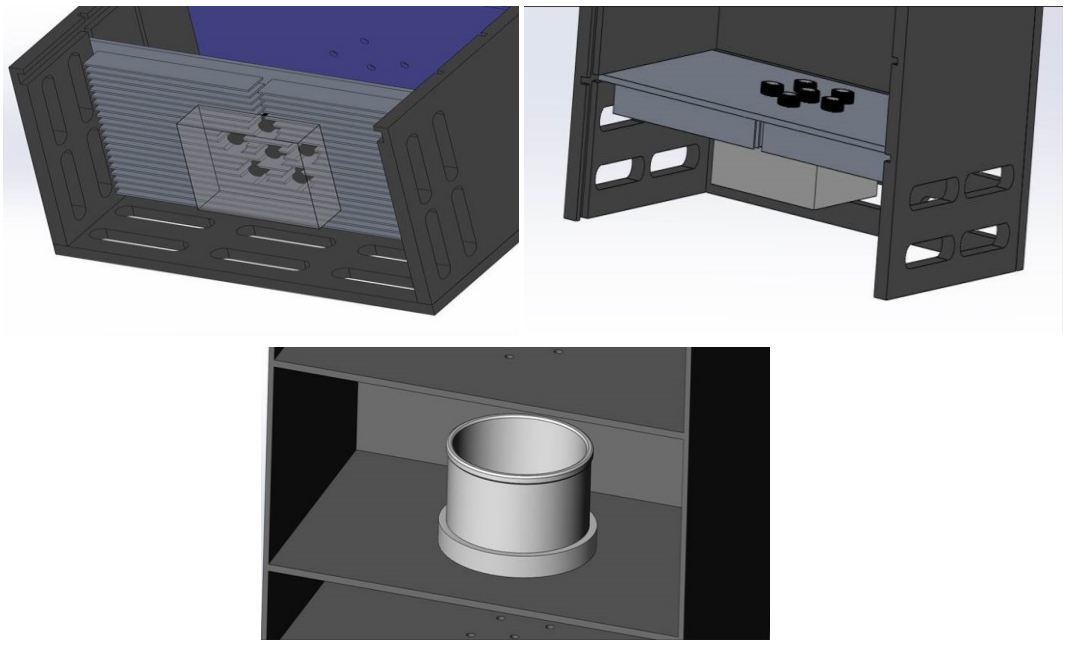

Figure 21: Model Drawings

As shown in the drawings, in the *figures 20 and 21*, the model was made with the idea of giving the chance to choose between multiple levels and distances from the camera, thus being able to find, following experiments, the one that best suited our needs. The various grooves on the sides of the structure allow the various plates to be inserted at adjustable distances with steps of 5 cm.

Figure 22: Model Side Picture

3.1.1 Power Supply System

Next to the structure itself, a power supply system for the LEDs and the cooling fan was also created. This system is equipped with the possibility of adjusting the luminous intensity of the LEDs by playing on the current delivered to each individual LED in order to better calibrate the instrument.

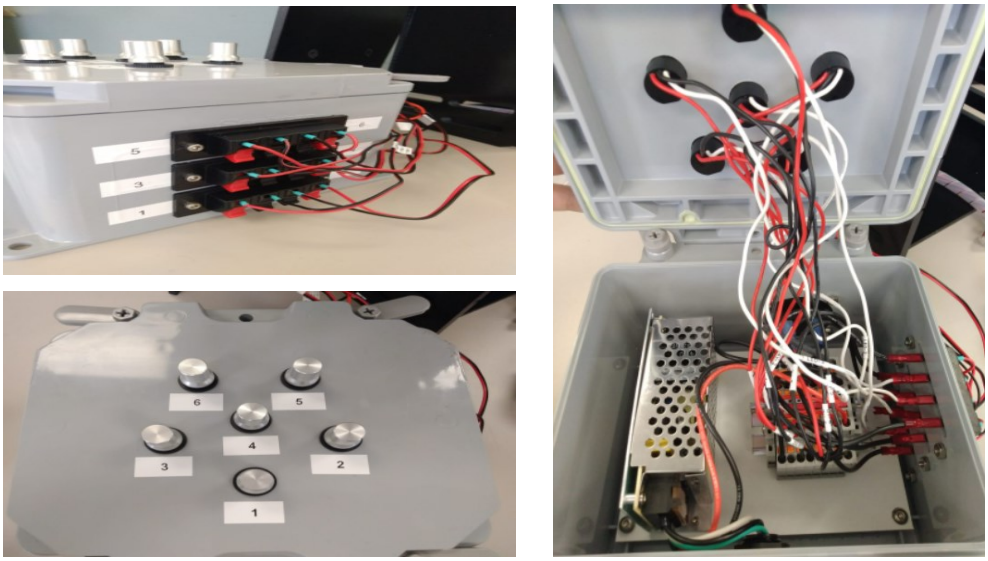

Figure 23: Power Supply Box

As shown in *figure 23*, the power supply has been positioned in a separate box to which all the LEDs and the fan are connected to. This generator has very specific characteristics:

- Input: AC 110/220V. 50/60Hz
- Output Voltage: DC 12V (Regulated by 10%)
- Output Current: Max 5A
- Output Wattage: Max 60W
- Safety Compliance: FCC / CE / RoHS / CCC
- Working Temperature: -10 °C to 60 °C
- Environmental Humidity: 10% - 95%
- Material: Aluminum, Electronic Components

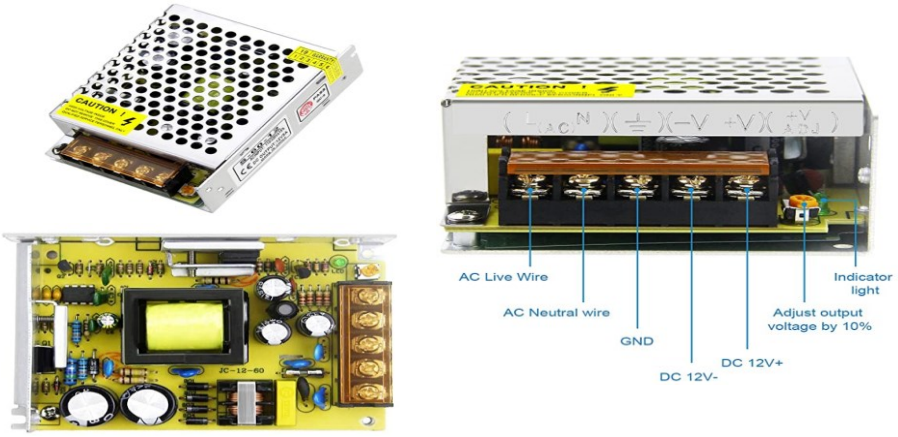

Figure 24: Power Supply Images

3.1.2 Cooling system

A very important part was ensuring proper and flicker-free operation of the LEDs. For this reason, one of the objectives was to ensure constant temperatures and that they did not exceed the threshold values for the LEDs. To do this, a cooling system based on two components was used for the plate on which the LEDs were positioned: a heat sink and a fan.

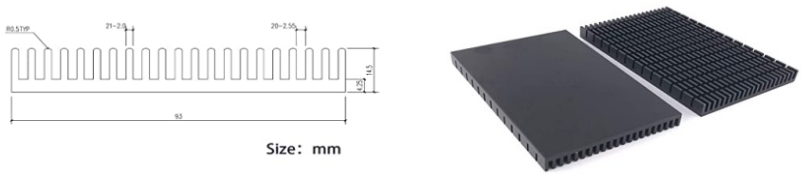

Figure 25: Heat Sink

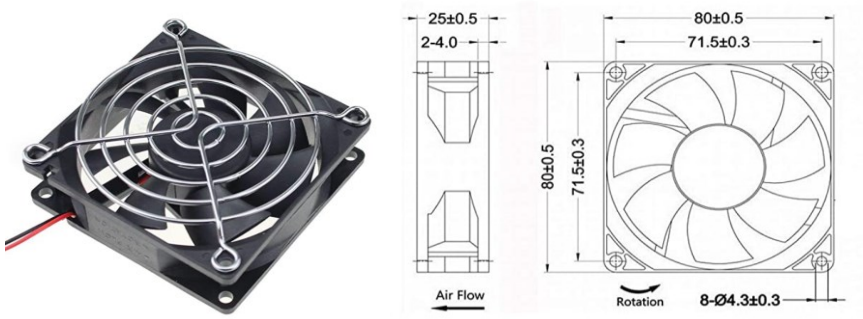

Figure 26: Fan

It should be noted that the ventilation system, positioned exactly under the LEDs, was mounted "upside down", with the fan facing downwards; this choice means that the air is not directed towards the LEDs but rather the air, heated by the LEDs in operation, is sucked outwards in this way the temperature does not undergo variations but remains almost constant over time.

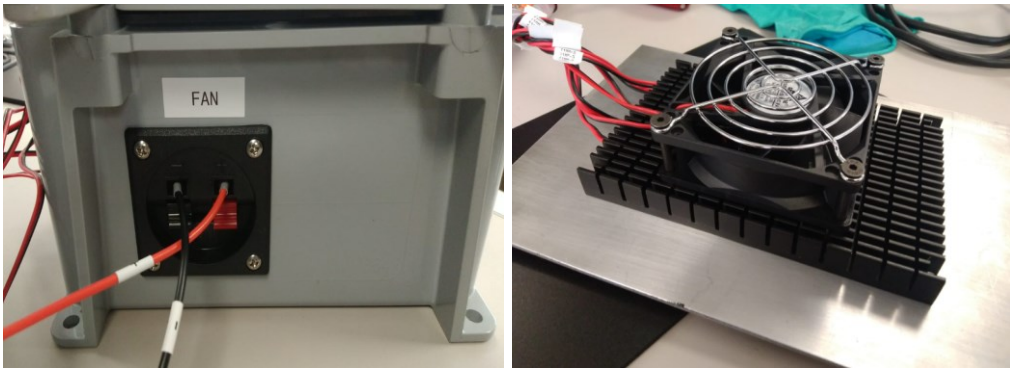

Figure 27: Cooling System

3.1.3 LEDs Lights

Another key component of the prototype are the LED lights; these lights were chosen following several attempts with different light sources to understand which were the most suitable for the needs of the project. The choice was influenced by several factors as the lights had to meet different requirements: space, heat emitted, wavelength emitted, brightness, etc. The research ended with the choice of LEDs proposed by *Oznium*. The latter have the possibility of various sizes (6 mm, 11 mm) and come with a very simple and effective method of mounting on surfaces. In fact, they just need a little hole in the structure of the right size feed the wires and led bolt through. Tighten the matching nut from the back side to make everything steady.

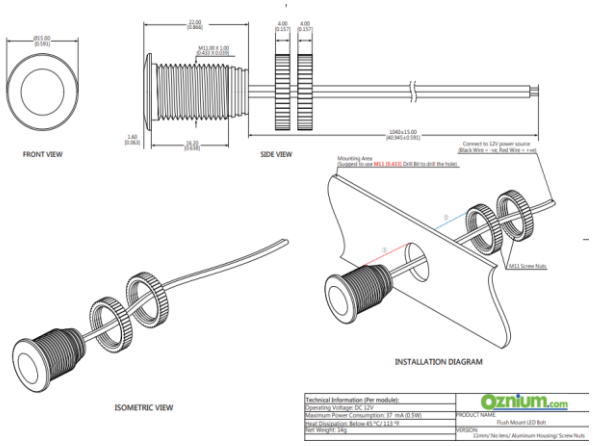

Figure 28: LEDs Drawings

So, in the *figure 28* above it is also shown how easy is mounting the LEDs light to the structure and for this reason also easy to change them in order to have different types; moreover, about the model, we decided to use six LEDs. This decision was made from an analysis to maximize the number of LEDs in the given structure. The purpose of using different LEDs lights is to have the possibility to make analysis, covering all the visible spectrum and also going to analyze UV light and its fluorescence phenomenon.

Version	LED Color	CCT(K)/Wavelength(nm)	Lumen(lm)	Current @ 12VDC (mA)
11mm/16mm	Cool White	9000K+	33	40
11mm	Neutral White	6000-6500K	33	40
11mm/16mm	Warm White	3000-3200K	33	40
11mm/16mm	Red	625	12	40
11mm/16mm	Green	525	25	40
11mm/16mm	Blue	470	4	40
11mm/16mm	Amber	595	8.5	40
11mm/16mm	UV	410	0.25	40

Dimmable	Yes
IP Rating	1W and 3W : IP68 fully waterproof / submersible
Polarity Sensitive	Yes
Operating Voltage Range	12 VDC
Heat Dissipation	Below 45C
Wire Gauge	Aluminum 1W: 22AWG red/black zip cord Stainless Steel 3W: 22AWG 2-core Marine Grade
Wire Length	1 meter (3.3 feet)
Housing	1W: Aluminum 3W: Stainless Steel
Lens	PMMA
Beam Angle	With Lens : 60 degree Without Lens: 180 degree
Weight	6mm: 6g 11mm, No Lens: 15.8g 11mm, With Lens: 16g 16mm, No Lens: 23.2g 16mm, With Lens: 23.6g Stainless Steel: 32.4g

Figure 29: LEDs Datasheet

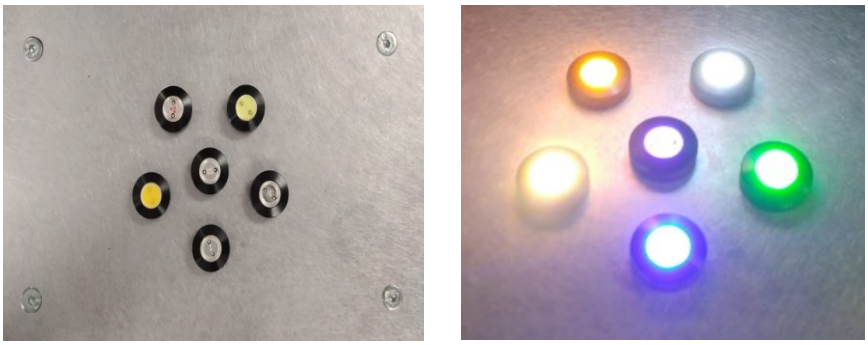

Figure 30: LEDs Shape and Colors

As shown in *figure 30* above, the LEDs have been arranged in a regular pentagon shape with one more in the center to maximize the number per occupied space. As shown, the LEDs chosen were:

LED Number	LED Color	CCT(K) / Wavelenght (nm)
1	Blue	470
2	Green	525
3	Warm White	3000 – 3200 K
4	UV	410
5	Cold White	9000 K
6	Amber	595

Table 3: LEDs Wavelength & Color

In addition, plates have been made to be inserted between the light source and the water layer and between the water and camera, to cut the light rays; these were made after several considerations both on the camera and on the distance from it. In fact, precisely on the realization of the latter and in order to have a perfect alignment between holes and light rays, it has been considered the distance between the plane and the LEDs, the fact that the camera, or rather the lens used, and the relative position of the collimating shutters. To make them, as well as an extremely precise machine to create the holes, it was necessary to consider the solid angle of view given by the chosen lens, equal to 43.4 ° and consequently the distances of the holes were adapted. The idea behind these shutters is to cut, if not all, most of the

diverging light rays, trying to keep only those perpendicular to the surface of the chamber and to the water, also reducing the phenomenon of refraction due to rays crooked.

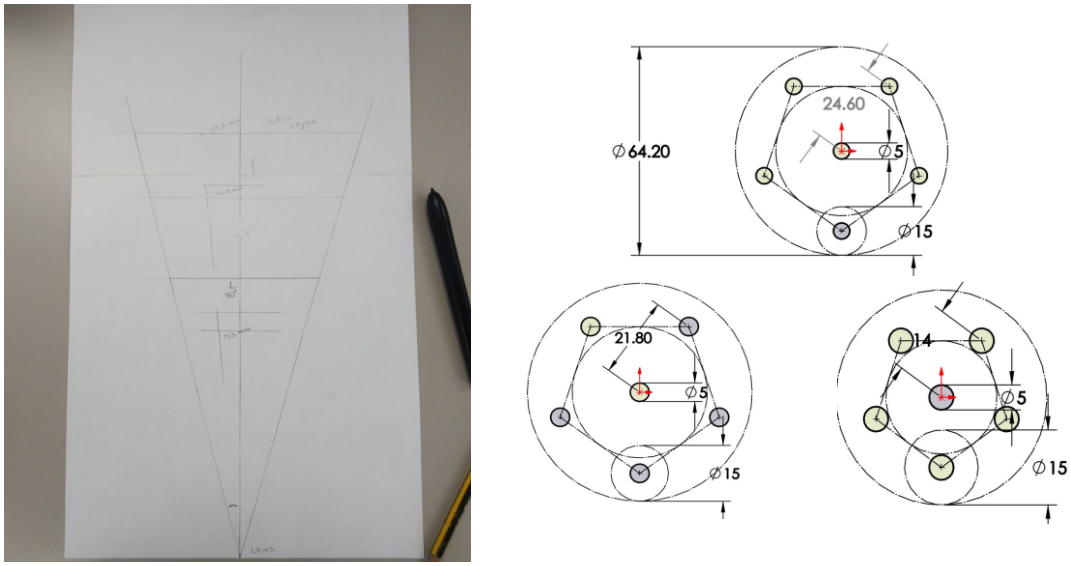

Figure 31: Collimating Holes Drawings

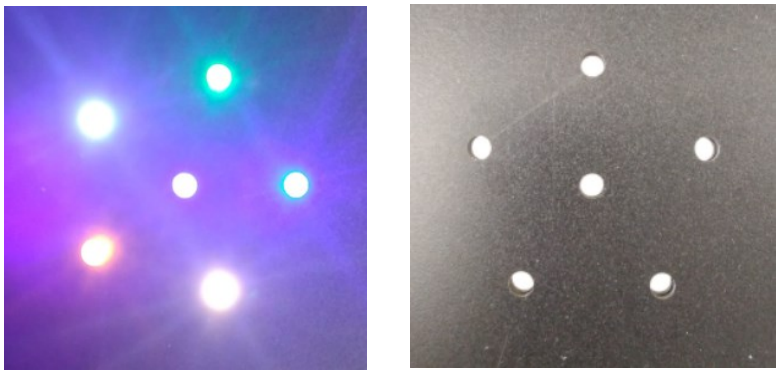

Figure 32: Alignment Holes-LEDs

As said before, the water with a precise thickness is placed in a borosilicate beaker glass. This container has an 8 cm diameter, and it is located on another aluminum plate that has a hole in the middle for the beaker itself in order to keep it stable and not let it move or shake.

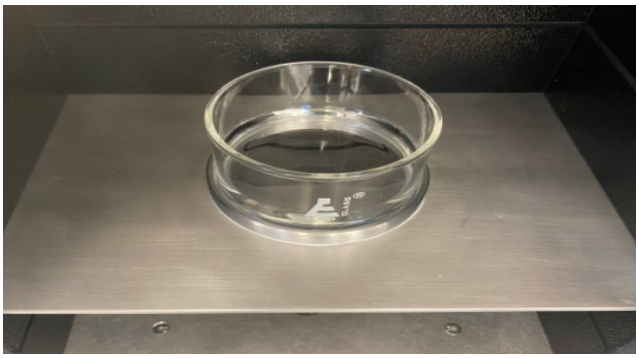

Figure 33: Beaker

Figure 34: Model Open

3.2 Camera

The heart of the model and project, intended as a sensor, is the camera itself that determines the mode and quality of the acquisition and how the images are taken. To make the choice a lot of variables have been considered: the budget was a concern, but the priorities have been all the proprieties of the camera and lens. Another aspect that has been considered in making the choice has been the actual chip shortage that have forced us to choose a camera and a lens that were already in stock to overcome the problem of a supply delay.

What has been chosen, it is a monochrome camera of Allied Vision, model *Alvium 1800 U – 2050*; this camera fits the needs and in the following pages are presented the characteristics of it using Allied Vision datasheet itself.

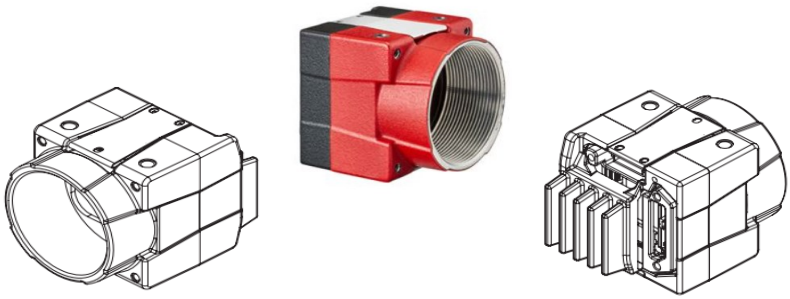

Figure 35: Alvium 1800U 2050

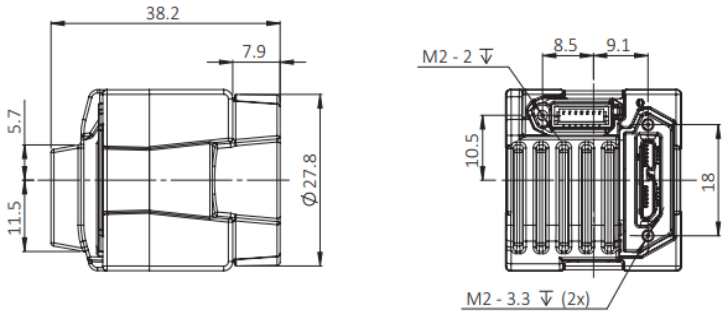

Figure 36: Alvium 1800U Lateral and Back View

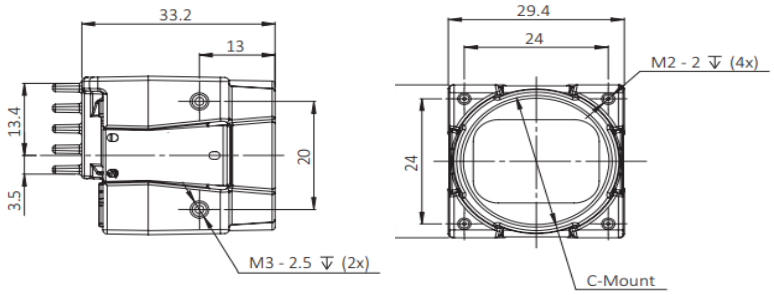

Figure 37: Alvium 1800U Lateral and Back View

The Allied Vision camera present itself as an industrial camera that is compact, low cost, it has got high performance design for machine vision and embedded applications.

Alvium 1800 U	**-2050**
Interface	USB3 Vision
Resolution	5496 (H) × 3672 (V)
Spectral range	300 to 1100 nm
Sensor	Sony IMX183
Sensor type	CMOS
Shutter mode	Global reset and Rolling shutter
Sensor size	Type 1
Pixel size	2.4 µm × 2.4 µm
Lens mounts (available)	C-Mount
Max. frame rate at full resolution	17 fps at ≥375 MByte/s, Mono8
ADC	10 Bit
Image buffer (RAM)	256 KB
Non-volatile memory (Flash)	1024 KB
Output	
Bit depth	Max. 10 Bit
Monochrome pixel formats	Mono8, Mono10
YUV color pixel formats	YCbCr411_8_CbYYCrYY, YCbCr422_8_CbYCrY, YCbCr8_CbYCr
RGB color pixel formats	BayerGR8, BayerGR10, BayerGR10p, BGR8, RGB8
General purpose inputs/outputs (GPIOs)	
TTL I/Os	4 programmable GPIOs
Operating conditions/dimensions	
Operating temperature	+5 °C to +65 °C housing temperature
Power requirements (DC)	Power over USB 3.1 Gen 1 | External power 5.0 V
Power consumption	USB power: 3.2 W (typical) | Ext. power: 3.4 W (typical)
Mass	15 g (bare board)
Body dimensions (L × W × H in mm)	13 × 26 × 26 (bare board, standard), 13 × 30 × 26 (bare board, 90°)
Regulations	2011/65/EU, including amendment 2015/863/EU (RoHS)

Figure 38: Alvium 1800U Datasheet

The *Alvium 1800U-2050* has been chosen for different reasons and most of them were carried out by the sensor mounted on the camera: *SONY IMX183 CLK-J*

3.2.1 Camera Sensor

This sensor, *SONY IMX183 CLK-J*, created by *Sony Semiconductor Solutions Corporation* is the heart of the camera and the project itself. A key point of this camera is the monochromatic view which gives the camera a much more sensitivity to light changes as explained in *section 2.3.2*.

It uses a high-sensitivity back illuminated structure 2.4 µm square unit pixel. The optical size is Type1 to enable use of *C-Mount lens*.

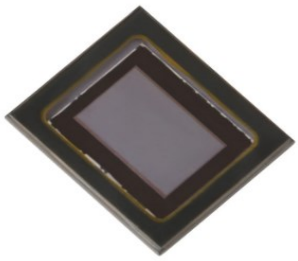

Item		IMX183CLK-J/CQJ-J
Output image size		Diagonal 15.86 mm (Type 1) aspect ratio 3:2
Number of effective pixels		5544 (H) × 3694 (V) approx. 20.48M pixels
Unit cell size		2.4 µm (H) × 2.4 µm (V)
Optical blacks	Horizontal	Front: 48 pixels, rear: 0 pixels
	Vertical	Front: 16 pixels, rear: 0 pixels
Input drive frequency		72 MHz
Output Interface		Sub-LVDS (576 Mbps / ch, Max.10 ch) *1
Package		118-pin LGA
Supply voltage V_{DD} (Typ.)		2.9 V / 1.8 V / 1.2 V

Item		Value	Remarks
Sensitivity (monochrome)	Typ. [F8]	388 mV	1/30s accumulation
G Sensitivity (color)	Typ. [F5.6]	461 mV	1/30s accumulation
Saturation signal	Min.	942 mV	Tj = 60 °C

Figure 39: Sensor IMX183 CLK-J Structure Datasheet

One of the many reasons that brought us to this camera, as said before, has been the sensor and its high quantum efficiency and spectral response.

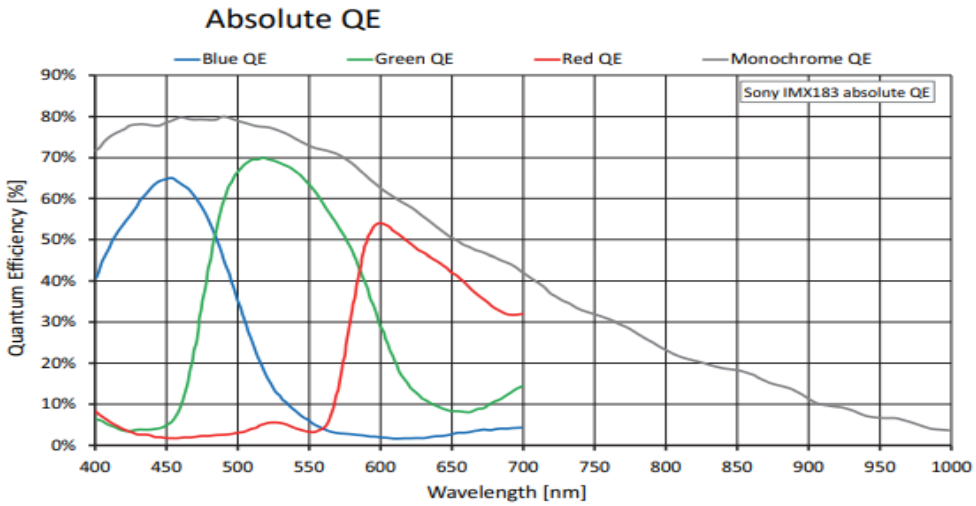

Figure 40: Sensor Quantum Efficiency (%)

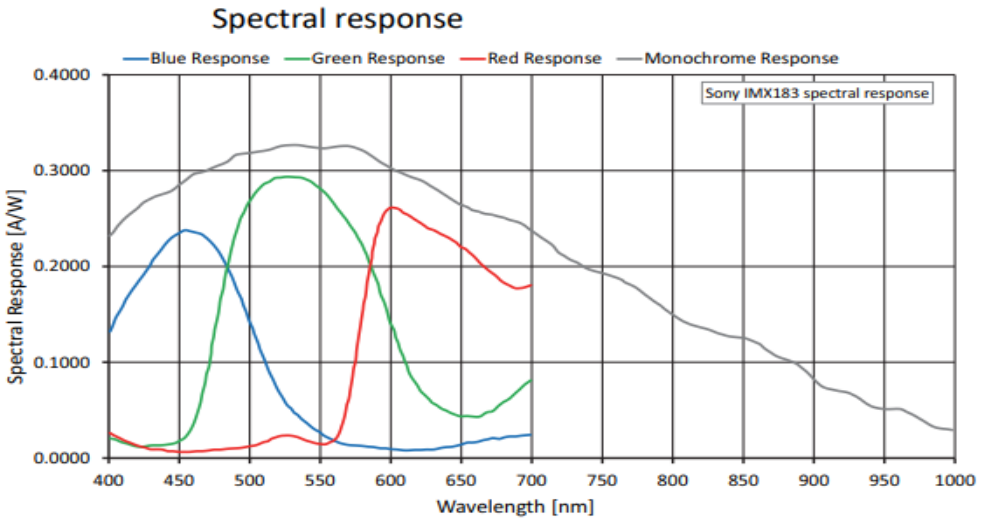

Figure 41: Sensor Spectral Response (A/W)

As shown in the *figures 40 and 41* the sensor *SONY IMX 183* presents higher peaks with the monochrome response and with a peak of 80 % for the absolute quantum efficiency. In addiction the sensor has a wide spectral range that goes from 300 to 1100 nm that allowed us to study not only the classic visible spectrum of lights but to investigate the infrared wavelengths and, more noteworthy, the first signs of ultraviolet that, as described in the *section 2.3.1*, carries more useful information.

Image format	Width [pixels]	Height [pixels]	ROI area [pixels]	Frame rate [fps]		
				450 MBps	375 MBps	200 MBps
Full resolution	5,496	3,672	20,181,312	21	17	9
HXGA	4,096	3,072	12,582,912	25	21	11
UHD 4K	3,840	2,160	8,294,400	35	29	16
QSXGA	2,560	2,048	5,242,880	37	31	17
WQHD	2,560	1,440	3,686,400	41	34	18
QXGA	2,048	1,536	3,145,728			
Full HD	1,920	1,080	2,073,600			
UXGA	1,600	1,200	1,920,000			
WXGA+	1,440	900	1,296,000			
SXGA	1,280	1,024	1,310,720			
HD 720	1,280	720	921,600			
XGA	1,024	768	786,432			
SVGA	800	600	480,000			
VGA	640	480	307,200			
QVGA	320	240	76,800			
QQVGA	160	120	19,200			
Maximum × half	5,496	1,836	10,090,656			
Maximum × minimum	5,496	8	43,968			
Minimum × maximum	8	3,672	29,376	21	17	9
Minimum × minimum	8	8	64	41	34	18

Figure 42: Alvium 1800U 2050 Image Format Information

As shown in the table above, and said before, the *Alvium 1800U-2050* has a maximum resolution of more than 20 million pixels in the full resolution format. The frame rate [*fps*] depends on the transmission speed. Using the cable *Micro-B Male to Type-A Male* it has to be considered a transmission speed of 375 MBps moreover.

3.2.1 Camera Lens

Another component it is obviously the camera lens; the lens for the camera is required to have focus and see.

Figure 43: TECHSPEC 16 Focal Length, HP Series Fixed Focal Length Lens

This lens, made by *Edmund Optics*, comes from a family of high-performance optical design (the *HP Series* family) and among the three customized optomechanical solution offered the HP series is the most adjustable version and it is the typical high quality machine vision lens.

The lens has been chosen after several considerations on different parameters that brought us to choose this lens. First of all, the sensor size of the camera that has been chosen, with a diagonal of 15,86 mm, has defined the type 1 lens; another aspect that had to be considered was the field of view, in terms of height and width of the water surface that should have been interrogated by the camera.

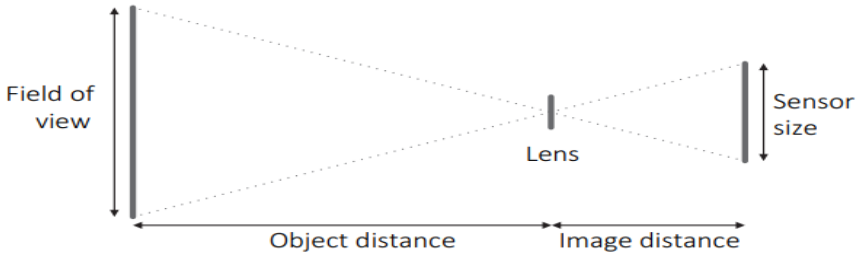

Figure 44: Field of View

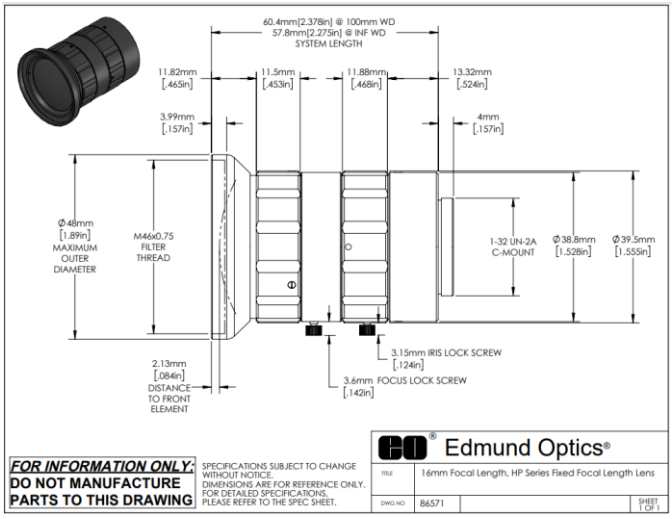

Figure 45: Lens Dimensions

Focal Length:	16mm
Minimum Working Distance[1]:	100mm
Focus Range[1] (lockable):	100mm – ∞
Length at Near Focus:	60.4mm
Length at Far Focus:	57.8mm
Filter Thread:	M46 x 0.75mm
Max. Sensor Format:	1"
Camera Mount:	C-mount

Aperture (f/#):	f/1.8 - f/16, lockable
Magnification Range:	0X – 0.13X
Distortion[2]:	<5%
Object Space NA[2]:	0.02
No. of Elements (Groups):	9 (7)
AR Coating:	¼λ. MgF_2@550nm
Weight:	195g

Sensor Size	½.5"	½"	⅓.8"	⅔"	Sony ⅔" *	1"	1" Sq[1]	⅘"
Field of View[3]	43.4mm - 19.9°	48.8mm - 22.3°	55.0mm - 25.0°	67.5mm - 30.4°	64.7mm - 29.2°	99.9mm - 43.4°	87.1mm - 38.5°	NA

Figure 46: Lens Datasheet

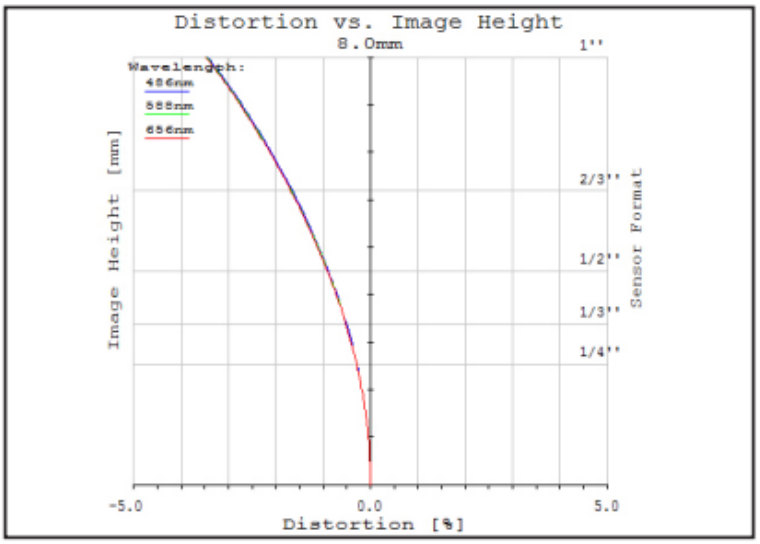

Figure 47: Lens Distortion on Image Height

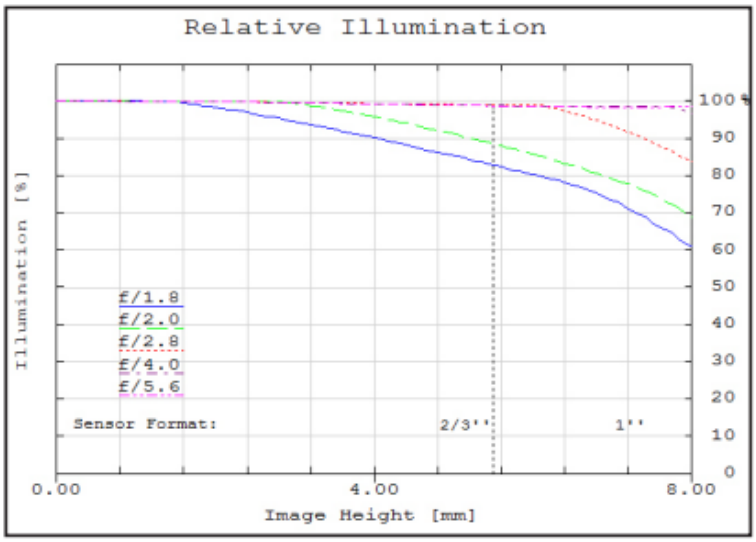

Figure 48: Lens Relative Illumination

3.2.3 MATLAB Connection

The *Alvium 1800U-2050* camera once connected to the computer via USB cable, it has the possibility to work with different software, first of all Vimba; this is presented as offered by the Allied Vision itself and it allows you to acquire images and also to work on the individual characteristics of the camera.

Figure 49: Allied Vision Vimba

What was used during the various experiments, however, it's the *MATLAB* environment and in particular the *MATLAB Acquisition Toolbox*, which the camera is compatible with.

Figure 50: MATLAB Logo

This choice of going to acquire the images directly in *MATLAB* is dictated by the fact that in this way, acquisition and processing and post processing of the images could take place in the same work environment, making the work easier and more consistent.

3.3 Instrument Calibration

This model represents a prototype for what it could be a new technology in wastewater field and as all the instruments it has been gone through a series of steps before it could have taken images and data to e analyzed. Hence, in order to calibrate the system different tests have been made to define the distance between the water layer, the LEDs and camera, other tests have been made to understand the water thickness to use throughout the experiments and also the parameters for the camera and LEDs' lights intensity.

3.3.1 Distance Choice

The distance between the various elements of the model, camera, LEDs lights and water, was the subject of several considerations before reaching a definitive choice for the experiments. Since it was possible to choose between different distances, after several attempts we came to the choice of placing the plate of LEDs at 31 cm away from the lens of the camera (fourth groove) and the plate, holding the beaker with the water, two shelves above, 10 cm from the light sources and consequently 21 cm from the lens.

This choice was dictated, as mentioned, by several factors; one bound was the working distance defined by the chosen lens which it must be more than 10 cm. Another factor was the field of view itself; having the chance of defining a *Region Of Interest* (ROI) manually it could have been possible to cut the black part on the edge, leaving only pixels to describe the LEDs, not losing information from the LEDs and at the same time making smaller frames that requires less memory.

3.3.2 Water Layer's Thickness Choice

To define a thickness with which to carry out the various experiments, different tests were made. The thicknesses adopted were from 0.5 cm up to 2.5 cm with intervals of 0.5 cm each. The tests were carried out with different samples of wastewater from the Greenway plant.

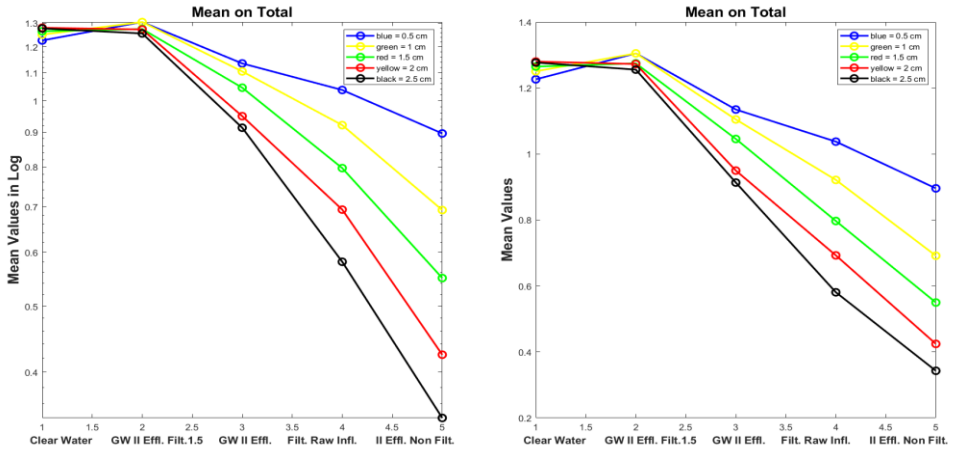

Figure 51: Results with Different Depth

The points on the graph are given by the average value of the values assumed by the individual pixels in the entire image. In *figure 51* we have the results plotted on the left in logarithmic scale and on the right in decimal scale and show a decreasing trend. In fact, starting from a situation of clean and drinkable water, one gradually passes to increasingly dirty and particle-laden wastewater. The decreasing trend, as you can see, is accentuated as the thickness of the water is bigger, as the light emitted by the LEDs has to pass through a thicker layer of water and is attenuated more.

Following these experiments, the choice was made to work with a water thickness of 1 cm, looking for a tradeoff between minimizing the thickness and maximizing the differences.

3.3.3 Test to Calibrate the System

Once the thickness and distance of camera and LEDs were determined, the system was calibrated using distilled water as a zero from which to start and have a reference.

The work was focused on some camera parameters and on the intensity of the light emitted by the LEDs. Of the many camera parameters that can be changed after several tests, it was understood that the ones that had the greatest influence were the exposure time, the gamma parameter, and the gain of the camera. Referring to the datasheets provided by the manufacturer, the gain parameter had to be kept as low as possible, possibly at 0 being this an amplifier, hence, not only of the signal but also of the possible noise. The gamma parameter is of fundamental importance as it affects several aspects of the frames; gamma

basically is a transformation curve that given an input, gives back an output and it is used as a compensation and as a correction of the values taken by the camera; it does not modify the contrast of the image but the perception of that giving the chance of better readability of darker spots. As for the exposure time and the power of the individual LEDs, individually adjusted via the dimmers, it was preferred to try to minimize the exposure time and maximize the power of the LEDs. This choice was also made to reduce the noise due to a higher exposure time and the decision to have LEDs that emit as many lumens as possible directed towards the water and the chamber.

All these parameters have been considered to obtain, with distilled water sample, values for each pixel that do not saturate the scale used. In this case, the camera *Alvium 1800 U – 2050* allows to have a 10 bits depth for representation of each pixel; this means that the grayscale doesn't go from 0 to 255 but it goes until 1023 giving a higher resolution and accuracy on light changes at the expense of a bigger request of memory to store the frames.

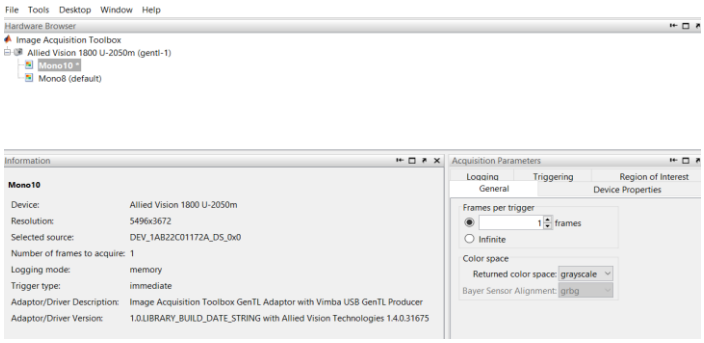

Figure 52: Mono10 Format

The choice of *mono10* format then forced the saving of the images as *Motion JPEG 2000 mjpeg2* which turns out to be a lossless compression format that is widely used in photography in fact, each frame is coded independently using JPEG 2000. This makes MJ2 more resilient to propagation of errors over time, more scalable, and better suited to networked and point-to-point environments.

The goal of the calibration carried out with distilled water is to obtain room parameters and LEDs that do not saturate the representation scale used to avoid later loss of information. To do this, the tests on the parameters were carried out in a cross-sectional way, looking for a solution that best fit the constraints described above.

For the individual LEDs, these tests were carried out by finding, with the same parameters set for the room, different solutions due to LEDs of different wavelengths but also of emitted lumens.

- *ROI*: 2176 1242 1256 1256
- *Time Exposure*: 331 µs
- *Gamma*: 2
- *Gain*: 0
- *Black Level*: 0

	Time Exposure				**Gamma**				**Power LEDs**			
	300µs	**1000µs**	**2500µs**	**4500µs**	**0.4**	**1**	**2**	**2.4**	**25%**	**50%**	**75%**	**100%**
300µs					-	-	+	X	+	+	+	+
1000µs					-	+	X	X	-	-	X	X
2500µs					-	X	X	X	X	X	X	X
4500µs					X	X	X	X	X	X	X	X
0.4	-	-	-	X					+	+	+	-
1	-	+	X	X					+	+	+	X
2	+	X	X	X					+	X	X	X
2.4	X	X	X	X					-	X	X	X
25%	+	-	X	X	+	+	+	-				
50%	+	-	X	X	+	+	+	X				
75%	+	X	X	X	+	X	X	X				
100%	+	X	X	X	-	X	X	X				

Table 4: Parameters Tests

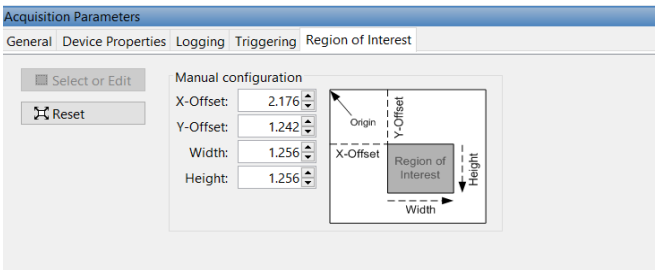

Figure 53: ROI Definition

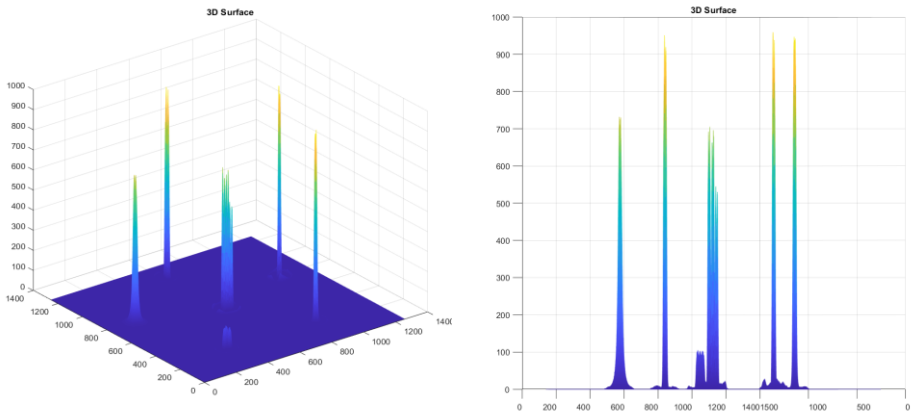

Figure 54: Distilled Water Calibration Values

3.3.4 Preliminary Test on Coffee Solution

Initially the first tests, to understand if the built system was working, were carried out on a solution of water and black coffee coming from the famous Canadian fast food restaurant chain, Tim Hortons. By recreating different solutions with well-known concentrations of coffee and water, some tests were made to see if the *Beer-Lambert law*, described in the *section 2.3.1*, was successfully verified.

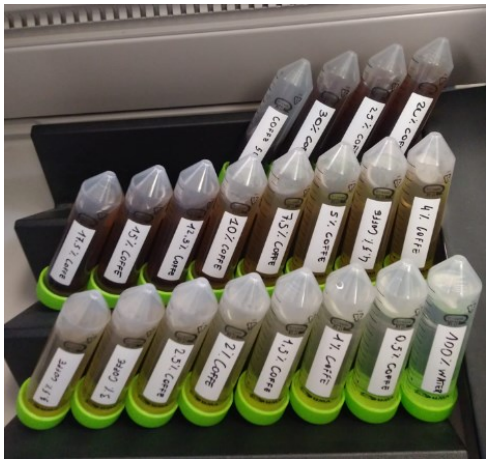

Figure 55: Coffee Samples

The *Beer-Lambert law* relates the attenuation of light to the properties of the material through which the light is traveling. The modern derivation of *the Beer–Lambert law* combines the two laws and correlates the absorbance, which is the negative decadic

logarithm of the transmittance, to both the concentrations of the attenuating species and the thickness of the material sample. The law is used for chemical analysis measurements and in physical optics, for photons, neutrons, or rarefied gases.

The results obtained are showed in the *figure 56* and it can be clearly seen on the left with logarithmic scale and on the right with a decimal scale the trend obtained by the system with samples with differences of 2.5% in coffee dilution.

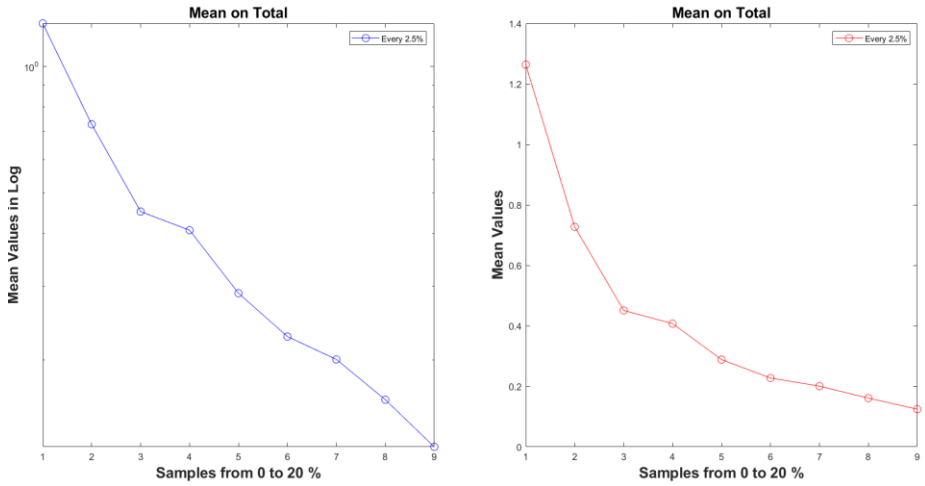

Figure 56: Values Plotted from Coffee Solutions

N LED	Variance Average over the samples
LED 1 Blue	$2{,}718 \cdot 10^{-7}$
LED 2 Green	$6{,}282 \cdot 10^{-6}$
LED 3 Warm White	$5{,}953 \cdot 10^{-5}$
LED 4 UV	$4{,}732 \cdot 10^{-5}$
LED 5 Cold White	$2{,}038 \cdot 10^{-6}$
LED 6 Amber	$4{,}847 \cdot 10^{-6}$

Table 5: Variance Average over the samples

3.4 Images Analysis

To analyze the images and define the samples, the system created each time acquired thousands of frames; in this way on the images, it was possible to calculate values such as mean and variance and to filter a noise component which was always present and could not be eliminated, although it was minimal compared to the reference values. As already mentioned in *section 3.2.3* the images were acquired with the MATLAB *Acquisition Toolbox* then were subsequently reprocessed to acquire the values of the total image and, after a segmentation operation, the values of the individual LEDs were acquired to be able to compare them individually.

First, the black noise of the camera has been calculated in order to be able to subtract it from the frames. Hence, once the camera was at working temperature, frames were acquired with the shutter on the lens to acquire completely black images that would have given the black noise value that we were interested in.

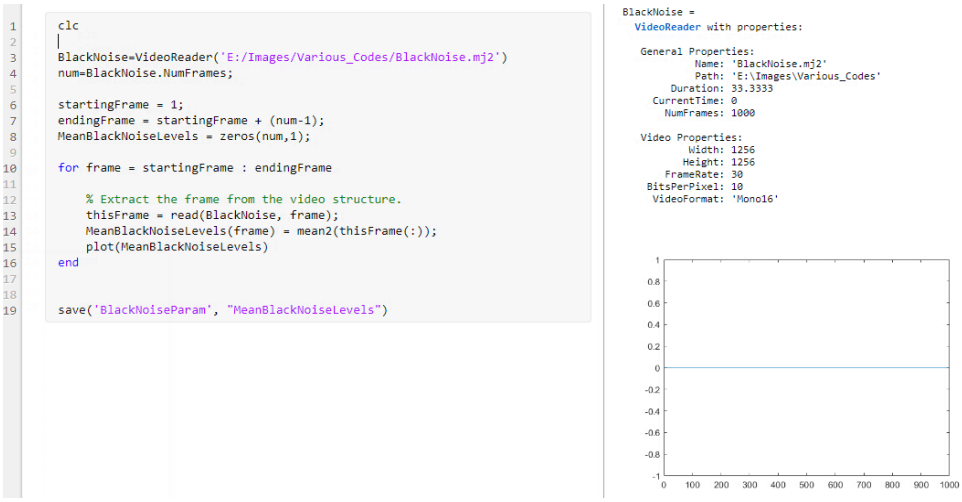

```
clc

BlackNoise=VideoReader('E:/Images/Various_Codes/BlackNoise.mj2')
num=BlackNoise.NumFrames;

startingFrame = 1;
endingFrame = startingFrame + (num-1);
MeanBlackNoiseLevels = zeros(num,1);

for frame = startingFrame : endingFrame

    % Extract the frame from the video structure.
    thisFrame = read(BlackNoise, frame);
    MeanBlackNoiseLevels(frame) = mean2(thisFrame(:));
    plot(MeanBlackNoiseLevels)
end


save('BlackNoiseParam', "MeanBlackNoiseLevels")
```

```
BlackNoise =
  VideoReader with properties:

  General Properties:
           Name: 'BlackNoise.mj2'
           Path: 'E:\Images\Various_Codes'
       Duration: 33.3333
    CurrentTime: 0
      NumFrames: 1000

  Video Properties:
          Width: 1256
         Height: 1256
      FrameRate: 30
   BitsPerPixel: 10
    VideoFormat: 'Mono16'
```


Figure 57: Black Noise Calculation Code

Because over several attempts the results were constantly zero and it has been decided to not subtract it from each frame because it was considered useless for the purpose of the analysis.

3.4.1 Image Segmentation

The images are first processed as a whole, calculating for each average of the values assumed by the pixels, standard deviation and variance of the values obtained; these operations are then carried out, after a segmentation shown in *figure 58*, also on the individual LEDs. Subsequently, the values obtained are filtered through a moving average filter to obtain even cleaner results with less oscillations.

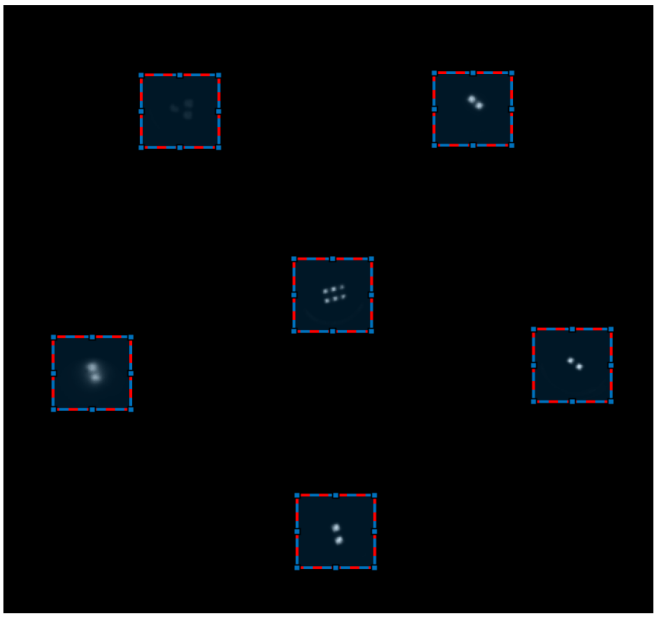

Figure 58: Segmentation of Each LED

Here, in the following figures we show some examples of plotting of results on some of the LEDs to make understand what the results have been.

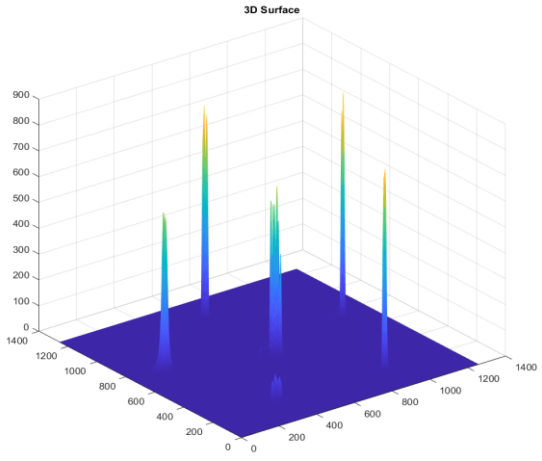

Figure 59: Plotting Entire Surface

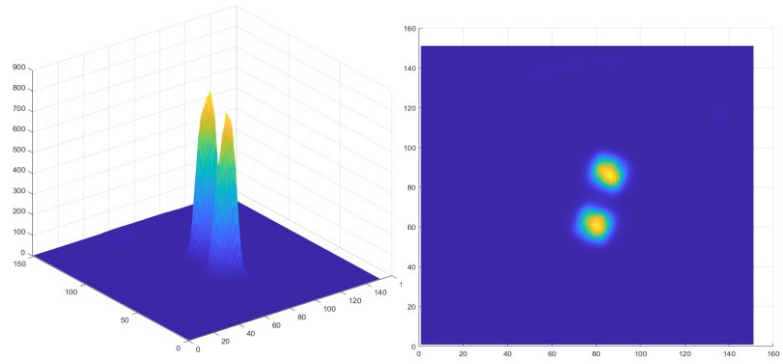

Figure 60: Plotting LED n1 Blue

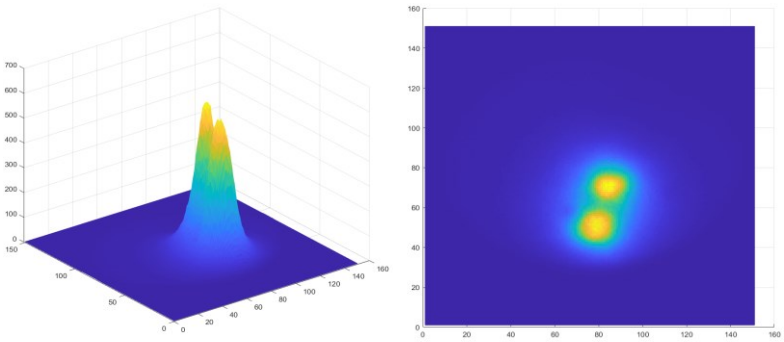

Figure 61: Plotting LED n3 Green

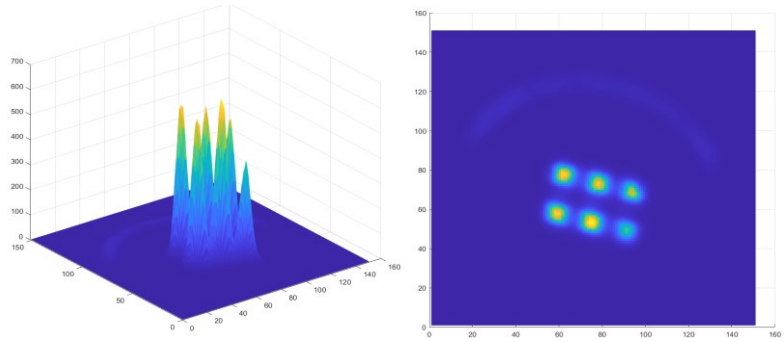

Figure 62: Plotting LED n4 UV

3.4.2 Data Extrapolation

As said before in the *section 3.4.1* once the images are segmented, the code applies the moving average filter created and calculate, for the entire image and each LED: the mean value, the variance and save all the variables and parameters in a file *.mat*.

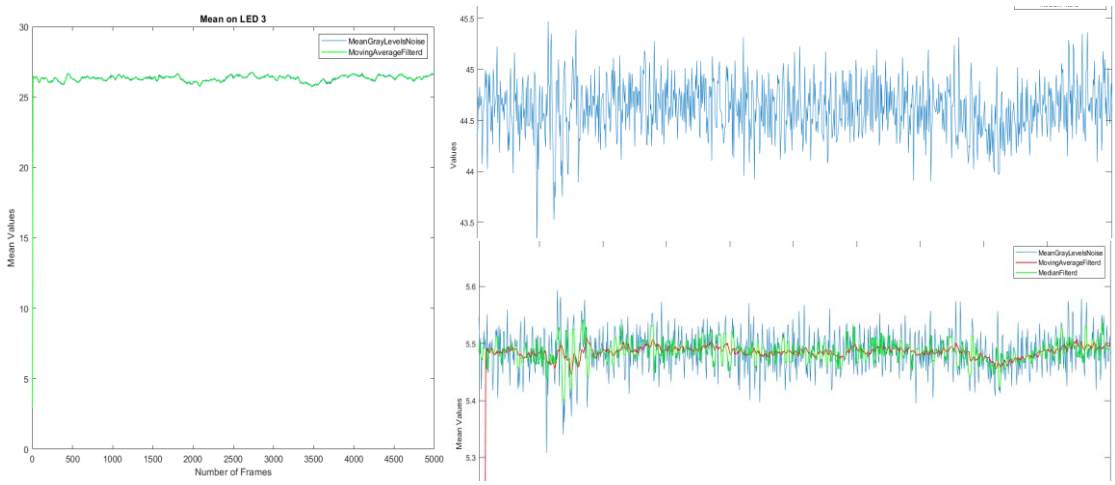

Figure 63: Example Data Plotting with Filter Application

3.4.3 Differences Analysis

To calculate and analyze the differences between the various wastewater samples, reference was made to another developed MATLAB code. About this, the parameters and values obtained and saved in the various .mat files are recalled in the workspace. In this case the differences are shown primarily through a plot of the various data obtained, which shows, *figure 64*, differences in the values due to a greater or lesser turbidity of the sample studied.

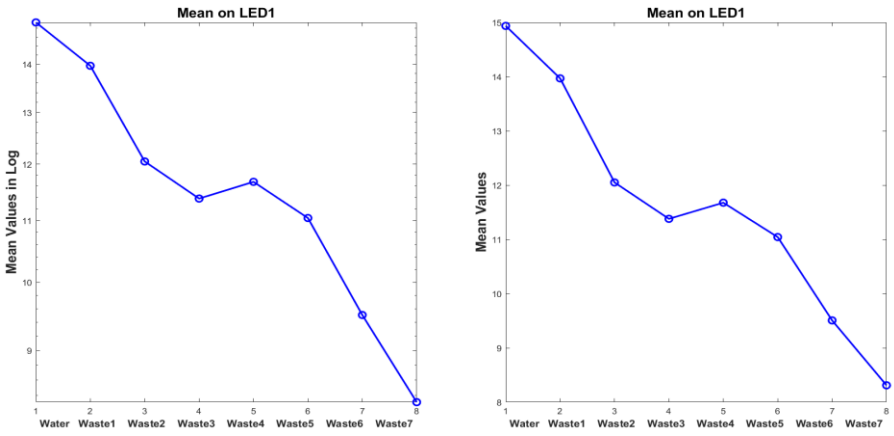

Figure 64: Plotting LED 1 Blue Values from Different Wastewaters

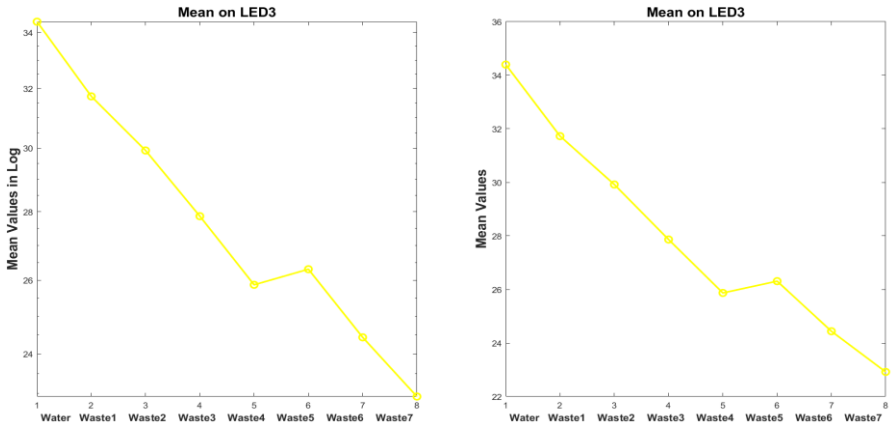

Figure 65: Plotting LED 3 Warm White Values from Different Wastewaters

The following plot has the aim to show how the system works over the different wastewater samples on each LED. What it can be understood from this plot is that, even if the differences on the same LED are small in terms of module, they are detectable and maintained over all the 6 LEDs, telling us that the system with all the LEDs can notice a difference.

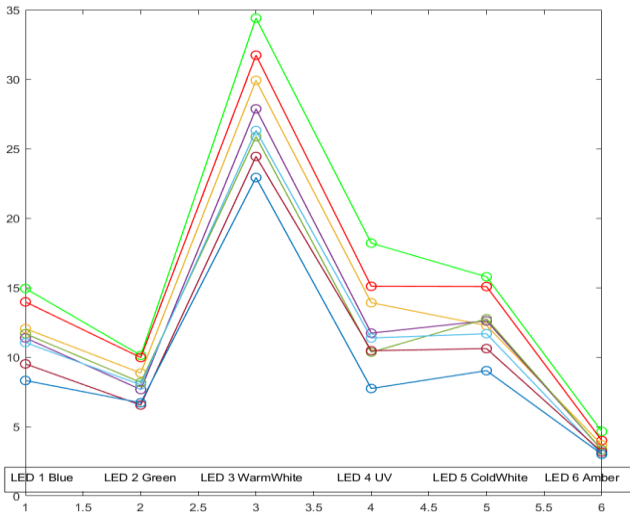

Figure 66: Plotting Values Over All LEDs

Another analysis on the differences was made using the functions used in *MATLAB Registration Estimator*.

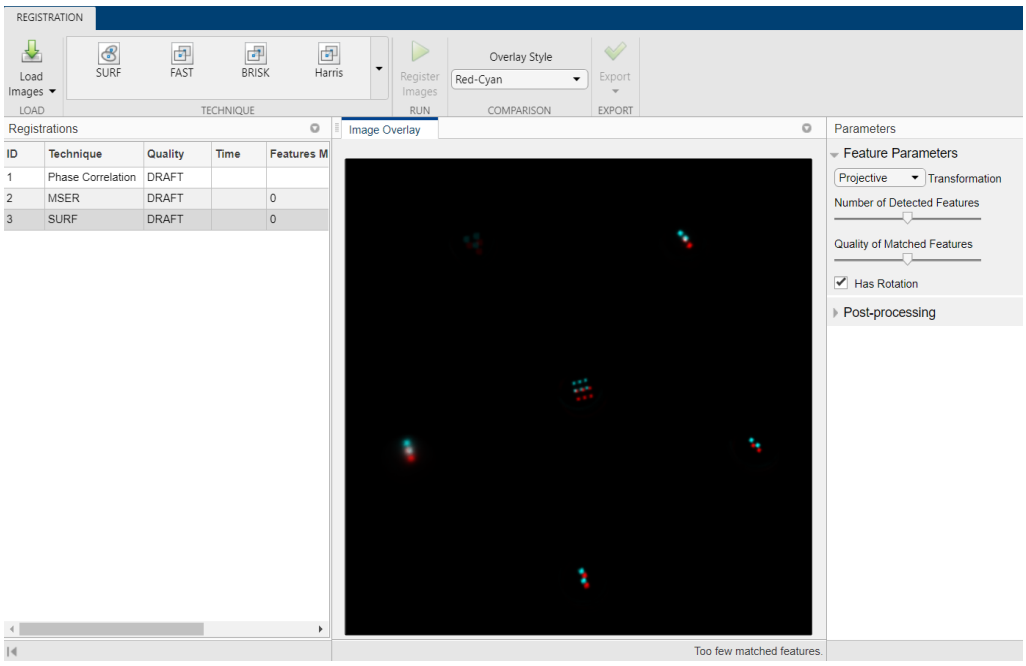

Figure 67: Registration Estimator

The toolbox is used to align the acquired images and thus be able to determine the difference pixel by pixel. After some tests, some parameters have been chosen to be used with the *imregister* function; place *imregconfig* ('monomodal'), *GradientMagnitudeTolerance* equal to 0.01 and define the minimum step and the maximum step and the number of iterations to find the alignment. With a for loop the differences were calculated between the different wastewater samples and then plotted.

```
[optimizer, metric] = imregconfig('monomodal');
optimizer.GradientMagnitudeTolerance = 0.01;
optimizer.MinimumStepLength = 1e-3;
optimizer.MaximumStepLength = 0.05;
optimizer.MaximumIterations = 100;

for ii=1:6

     align_W_W1{ii} = imregister(LEDWater{1,ii},LEDWaste1{1,ii},'rigid',optimizer,metric);

     DiffW_W1{ii} = double(align_W_W1{1,ii}) - double(LEDWaste1{1,ii});

     align_W1_W2{ii} = imregister(LEDWaste1{1,ii},LEDWaste2{1,ii},'rigid',optimizer,metric);

     DiffW1_W2{ii} = double(align_W1_W2{1,ii}) - double(LEDWaste2{1,ii});

     align_W2_W3{ii} = imregister(LEDWaste2{1,ii},LEDWaste3{1,ii},'rigid',optimizer,metric);

     DiffW2_W3{ii} = double(align_W2_W3{1,ii}) - double(LEDWaste3{1,ii});

     align_W3_W4{ii} = imregister(LEDWaste3{1,ii},LEDWaste4{1,ii},'rigid',optimizer,metric);

     DiffW3_W4{ii} = double(align_W3_W4{1,ii}) - double(LEDWaste4{1,ii});

end

surf(DiffW_W1{1},'EdgeColor',"flat")
surf(DiffW_W1{2},'EdgeColor',"flat")
surf(DiffW_W1{3},'EdgeColor',"flat")
surf(DiffW_W1{4},'EdgeColor',"flat")
surf(DiffW_W1{5},'EdgeColor',"flat")
surf(DiffW_W1{6},'EdgeColor',"flat")
```

Figure 68: Alignment MATAB Code

Another step in analyzing the collected data was to use two different *MATLAB* toolboxes for classification and regression modeling.

As regards the classification, the *Classification Learner* was used; this app trains models to classify data; it uses various supervised classifiers with machine learning and it allows automated training to search for the best classification model type including decision trees, nearest neighbors, network classification etc.

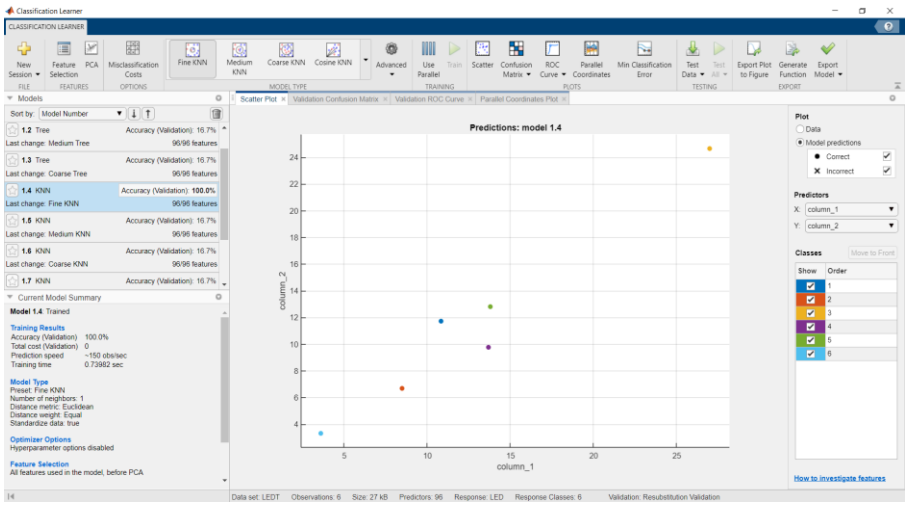

Figure 69: Classification Learner

About the prediction models it has been used the *Regression Learner* Toolbox; this app is used to train regression models to predict data, it can perform automated training too, to search for the best regression model type including linear regression models, regression trees, neural network regression models etc.

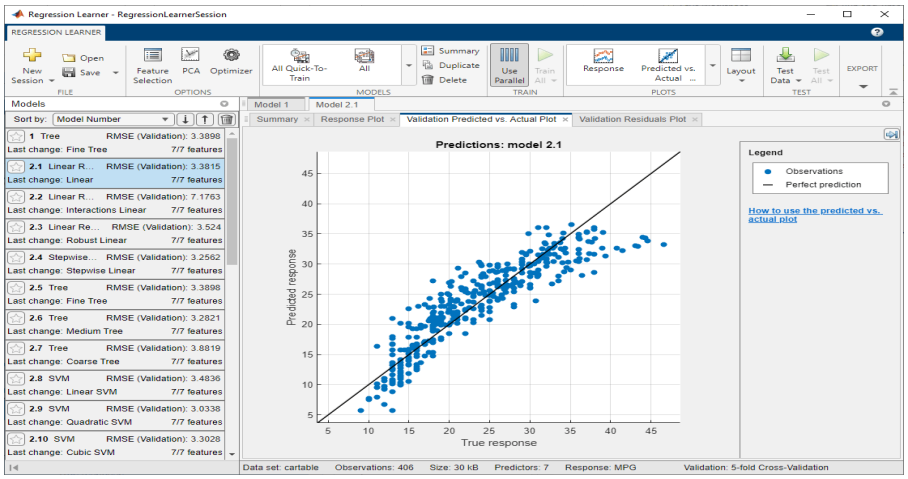

Figure 70: Regression Learner

Chapter 4 Experimental Results

4.1 Validation Experiments

To validate the system and how it works, the model was used to study wastewaters samples taken from the Ilderton wastewater plant. It has been taken hourly samples for four weekdays, from Monday morning to Friday morning, simulating how, in the future, the system would work. Moreover, the data collected by the system have been related to other two different instruments in order to have the possibility to track the results obtained and check if the system work properly. Hence, the data have been taken with a turbidimeter *2100Q* and a spectrophotometer *DR6000* from *Hach company* to measure the turbidity and the absorbance of each sample.

Figure 71: Hach Turbidimeter & Spectrophotometer

The purpose of having the data from these other well-known instruments is to see if the response of the new tool follows the one of instruments sold on the market, still used in the sector and worth thousands of dollars.

The wastewater samples were sampled through an autosampler placed in a tank of Ilderton wastewater plant, taking 24 samples per day of a secondary effluent. The instrument, showed in *figure 72*, was programmed to sample water every hour.

Figure 72: Autosampler

Figure 73: Ilderton Wastewater Plant

4.1.1 Scattering Experiment

This experiment has been done to proof the concept of the scattering phenomenon explained above in the *section 2.3.1*. To do so, the beaker has been modified with some black velvet pads. These pads have the purpose of blocking the direct light rays coming from the LEDs and let the camera see only the scattering phenomenon due to particles present in the water.

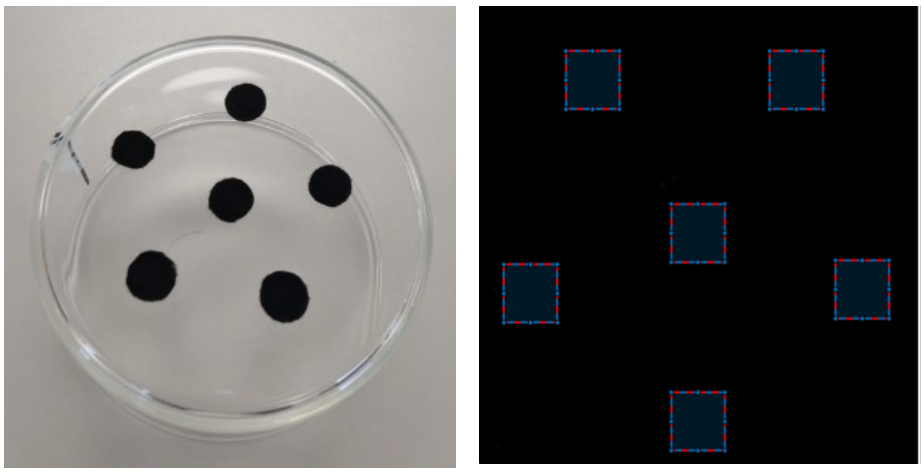

Figure 74: Beaker with Black Pads

For this experiment different samples have been chosen from the ones taken from the Ilderton wastewater plant. The samples considered has been the ones that registered the highest values with the turbidity test:

- Thursday 9 pm 15.12 NTU
- Thursday 10 pm 12.09 NTU
- Thursday 11 pm 10.43 NTU
- Friday 8 am 17.4 NTU

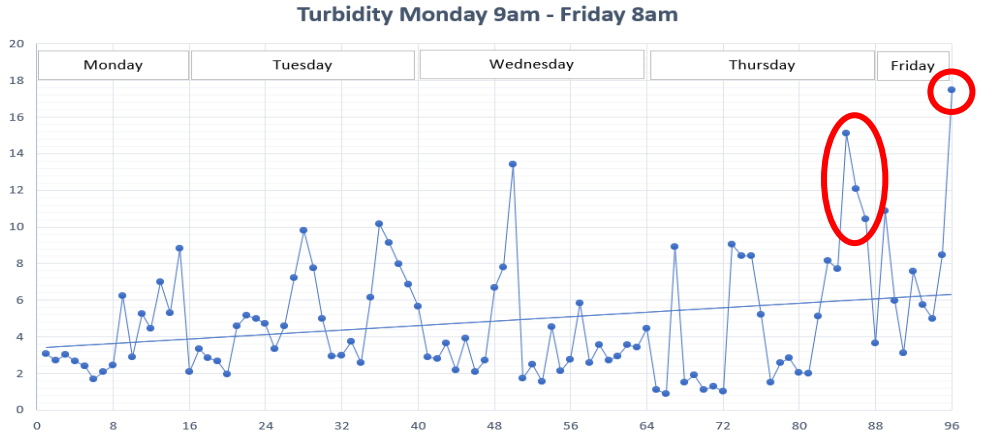

Figure 75: Values Chosen

4.2 Results from the Hourly Sampling

In this section it will be shown the results obtained with the experiments performed during the last weeks. The focus has been on the results produced by the hourly sampling of the Ilderton wastewater plant and on the scattering experiments.

4.2.1 Turbidimeter Results

The results from the turbidimeter have been obtained with three measurements for each sample.

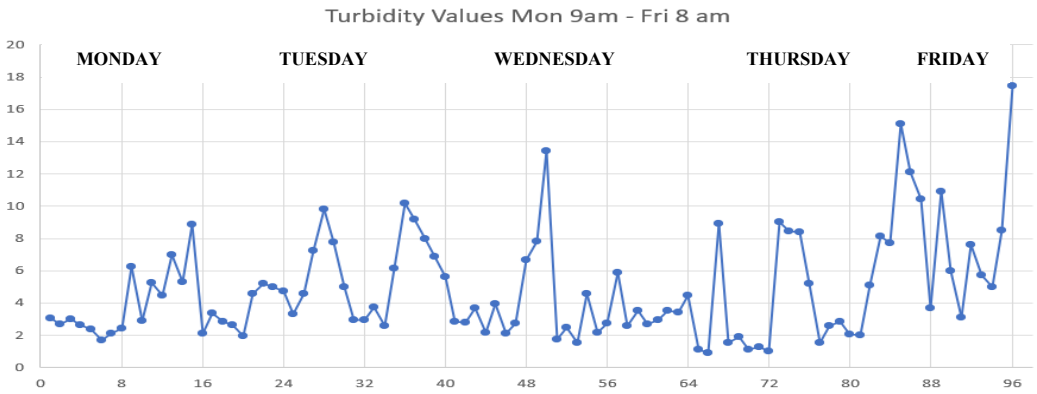

Figure 76: Results on Turbidity Mon 9am – Fri 8am

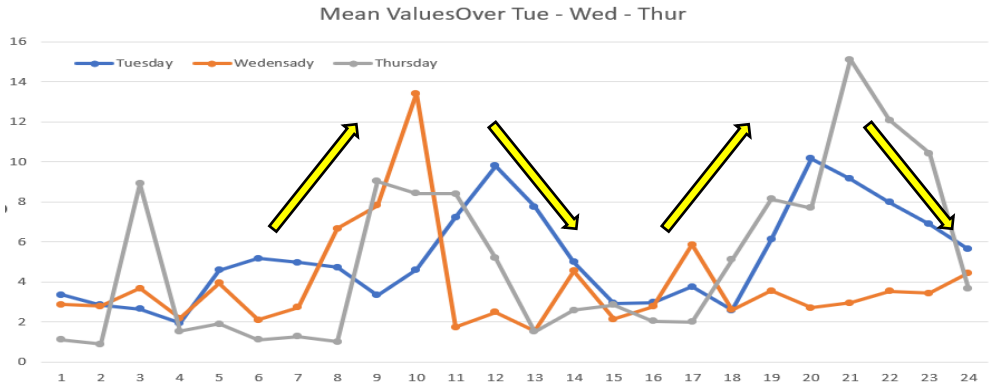

Figure 77: Results on Turbidity Tuesday to Thursday

In the second plot, the data collected over the three full days of sampling have been compared in order to understand and see if there were trends or patterns. As it is shown in the *figure 78*

77, there are two trends recognizable during a day, with values of turbidity that increase from 9 am to 12 am and again from 8 pm to 11 pm.

4.2.2 Spectrometer Results

The results of the spectrometer were analyzed in different ways, both by looking at the individual wavelengths and by looking at the integral value of the absorbance curves of each sample.

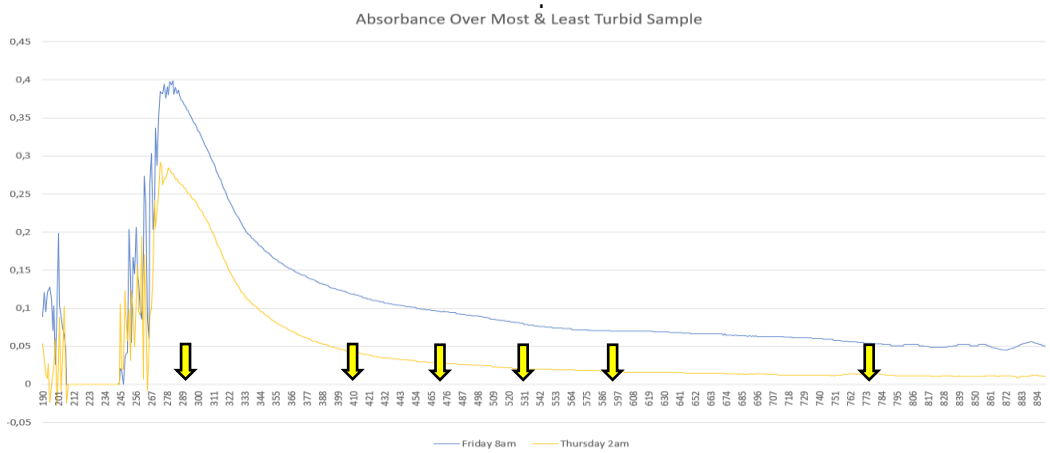

Figure 78: Absorbance Value Thur 2am & Fri 8am

As expected, the absorbance values on the spectrum analyzed, from 190 nm to 900 nm of the two most different samples turn out to be quite different. On all the spectrum the wavelengths that have been chosen for a more accurate analysis are the ones related to the LEDs used in the system; they were considered in particular across the spectrum in order to be able to compare results and see if there were trends or patterns that were similar. Alongside the values described, other values have been taken into consideration, 290 nm and 780 nm, and above all the integral value of the absorbance curve has been considered, to have a more general point of view.

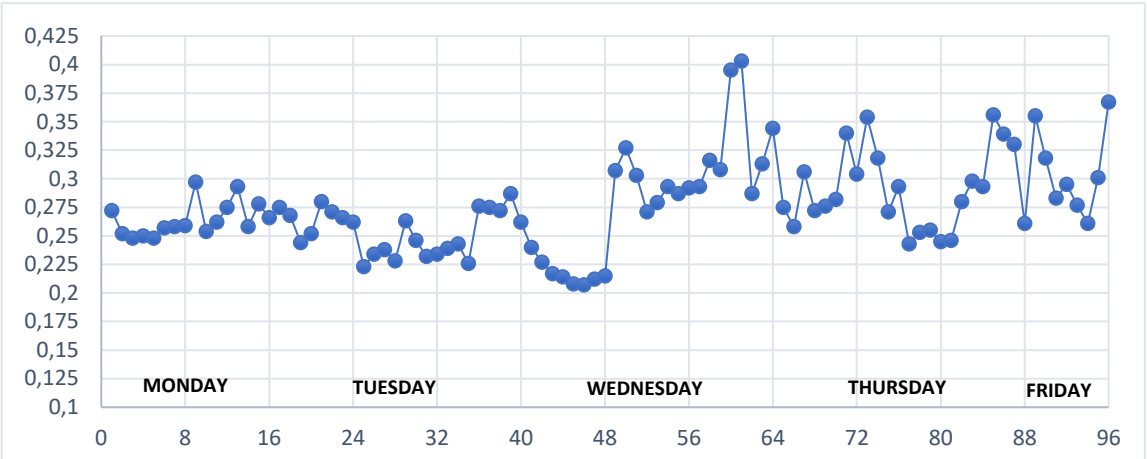

Figure 79: 290 nm Absorbance Values

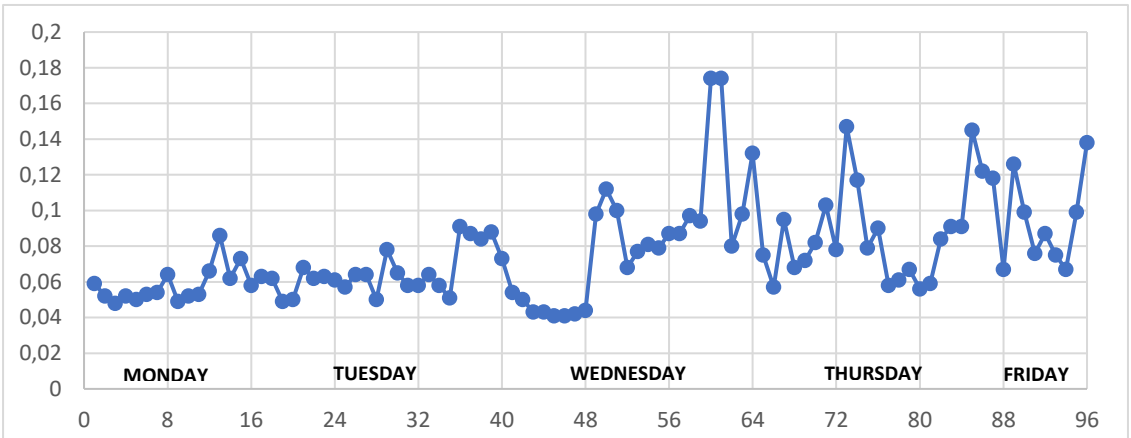

Figure 80: 410 nm Absorbance Values

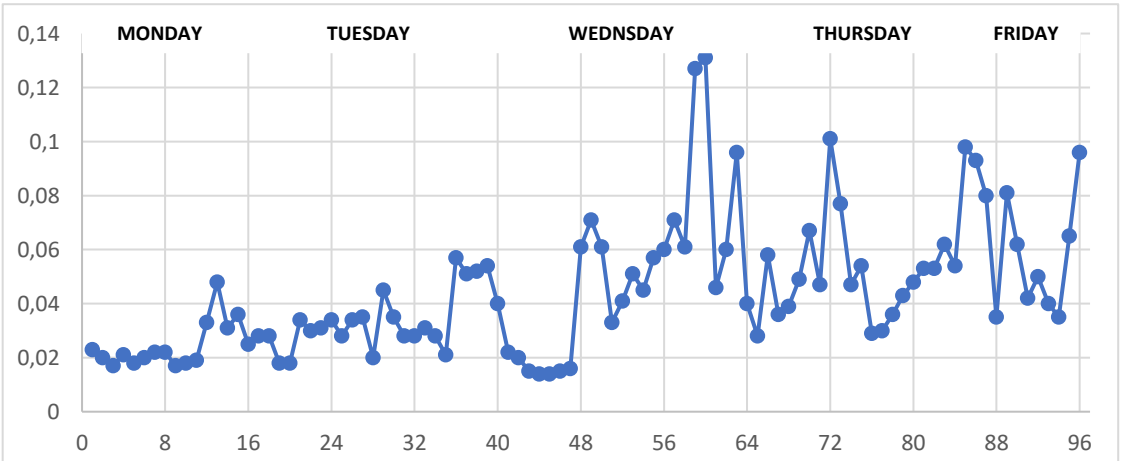

Figure 81: 470 nm Absorbance Values

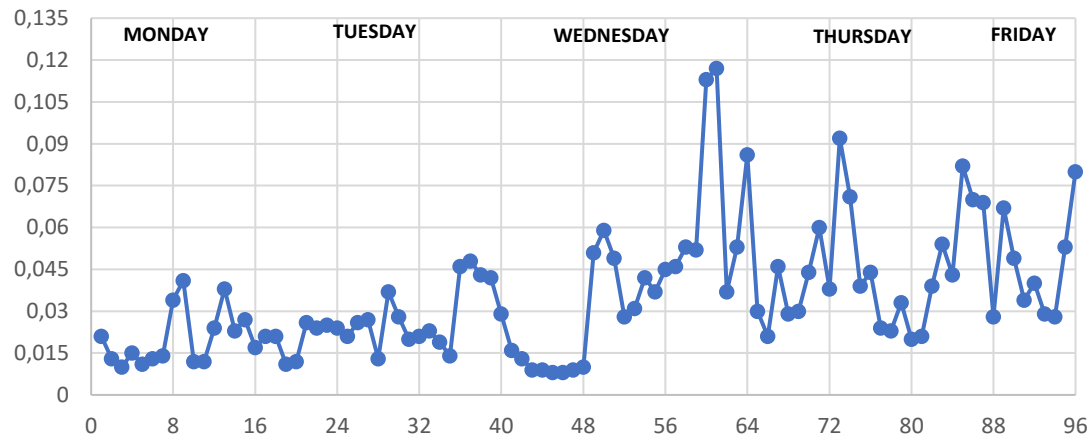

Figure 82: 530 nm Absorbance Values

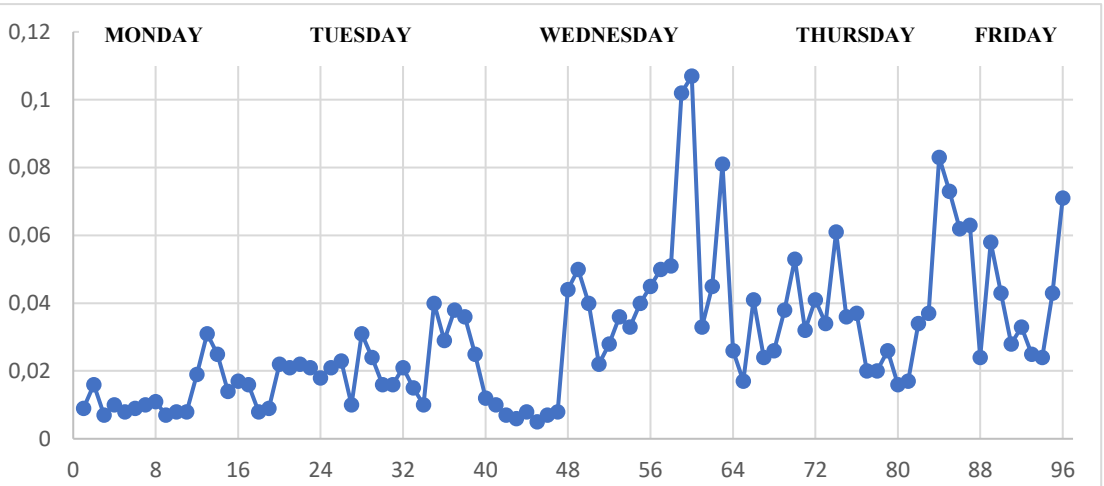

Figure 83: 590 nm Absorbance Values

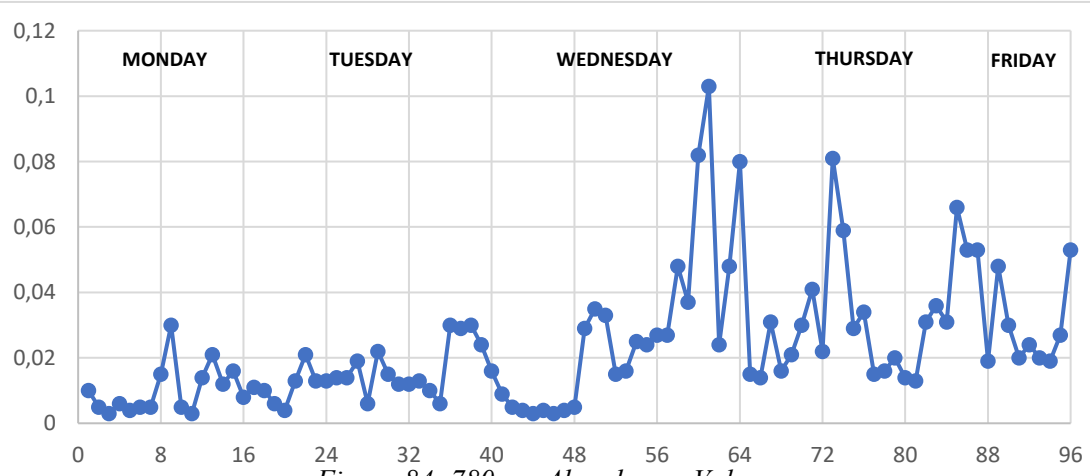

Figure 84: 780 nm Absorbance Values

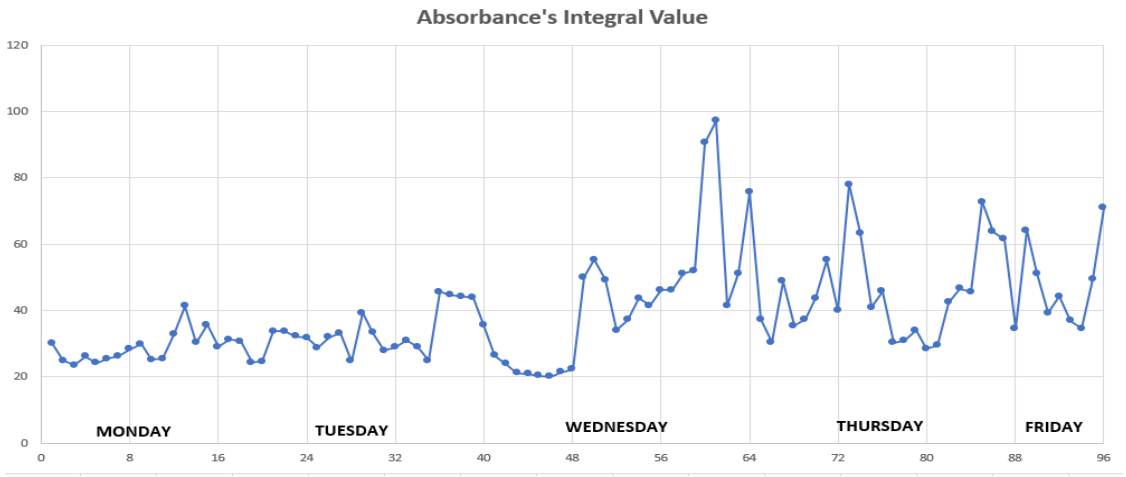

Figure 85: Results on Absorbance Curves

As showed in the figures above, the trend over the results of the spectrophotometer is pretty much the same; the main differences are the values, in terms of absolute value, that the absorbance assumes.

4.2.3 Camera System Results

The camera system results related to each LED are showed in the following figures. The variance, calculated on the measurements made by the new system created, was not shown on the graph as it cannot be graphically detected as it is always at least two orders of magnitude lower than the values obtained in the measurements.

N LED	Variance Average over the samples
LED 1 Blue	0,0014
LED 2 Green	0,0017
LED 3 Warm White	0,0012
LED 4 UV	0,0021
LED 5 Cold White	0,0012
LED 6 Amber	0,0016

Table 6: Variance Average over the samples

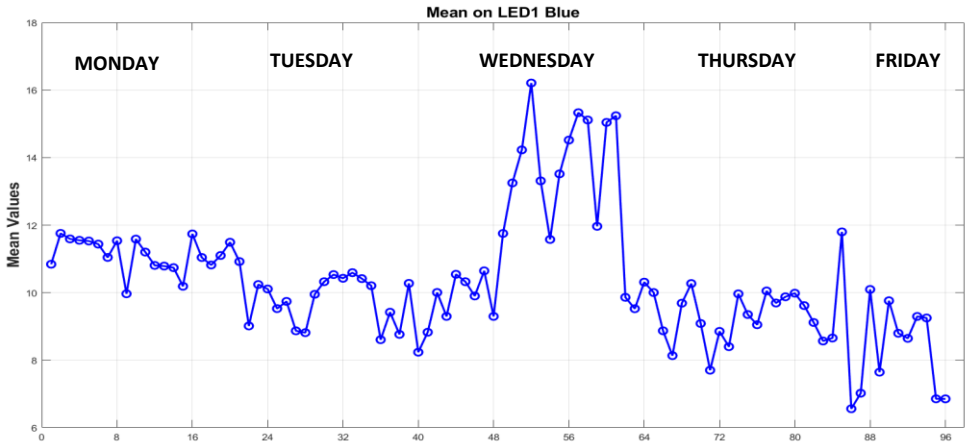

Figure 86: Results on LED 1 Blue

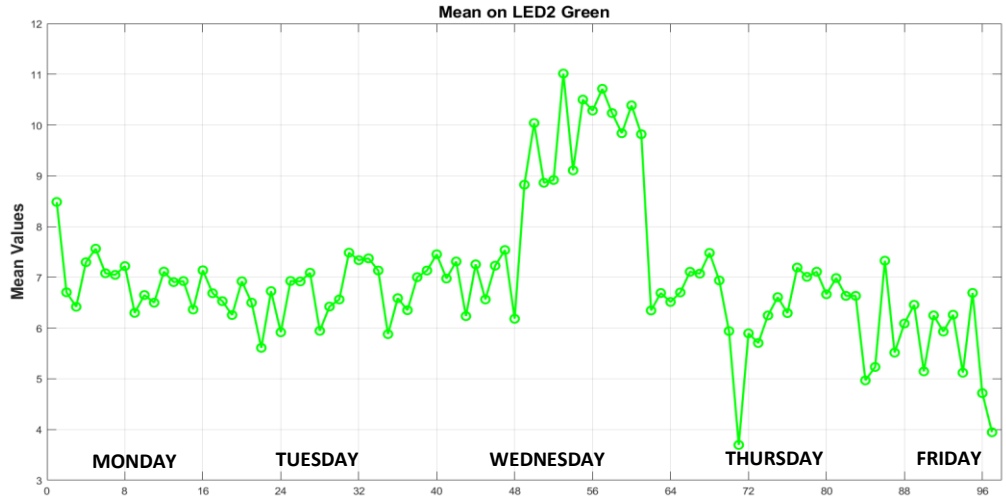

Figure 87: Results on LED 2 Green

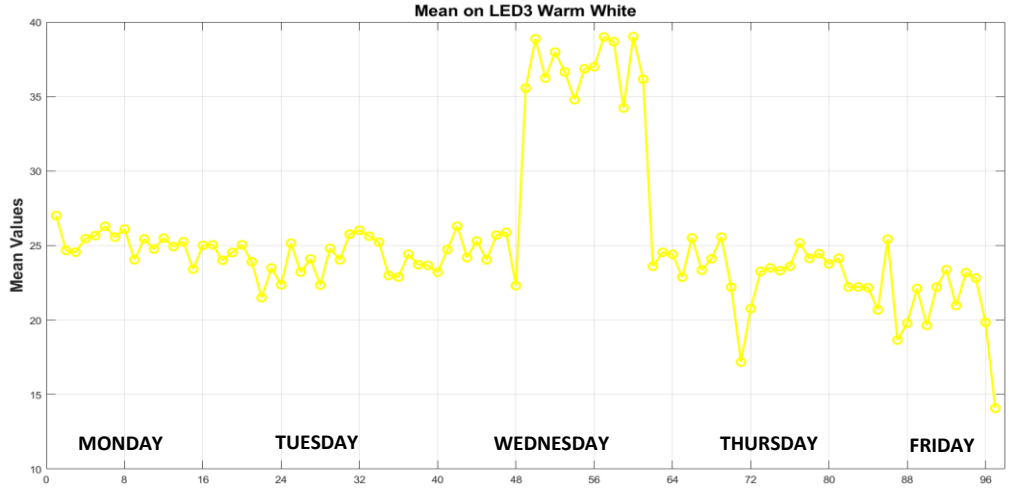

Figure 88: Results on LED 3 Warm White

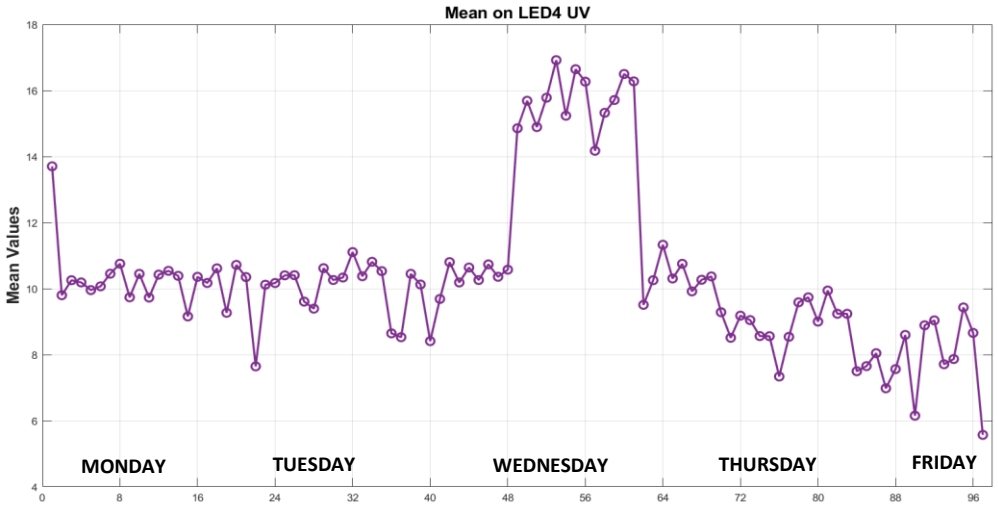

Figure 89: Results on LED 4 UV

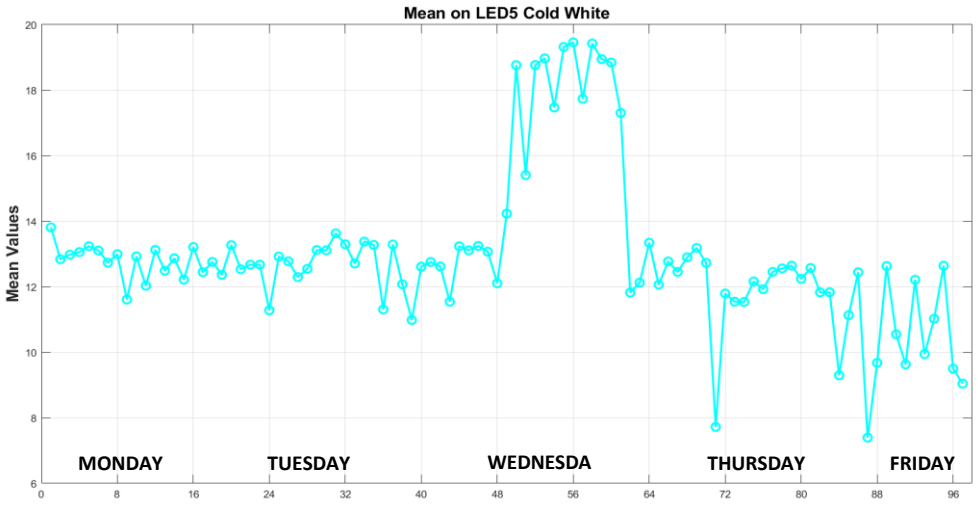

Figure 90: Results on LED 5 Cold White

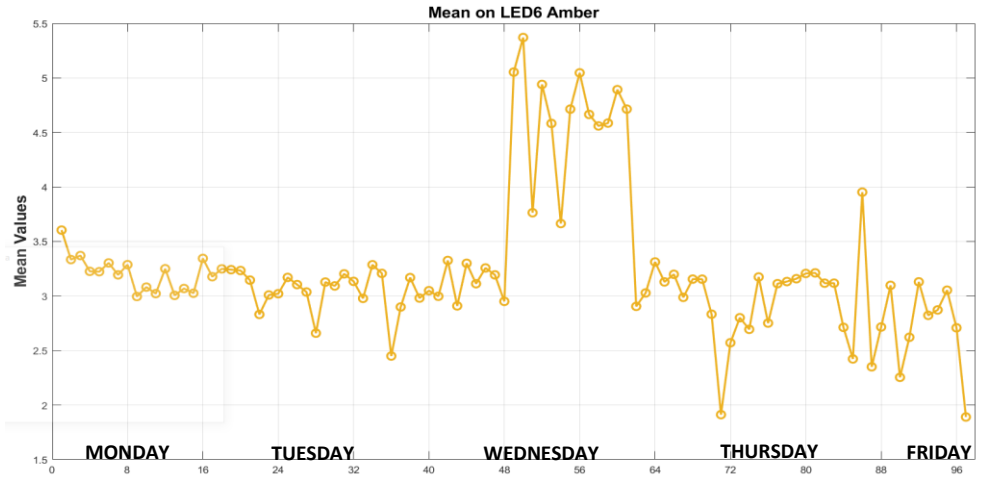

Figure 92: Results on LED 6 Amber

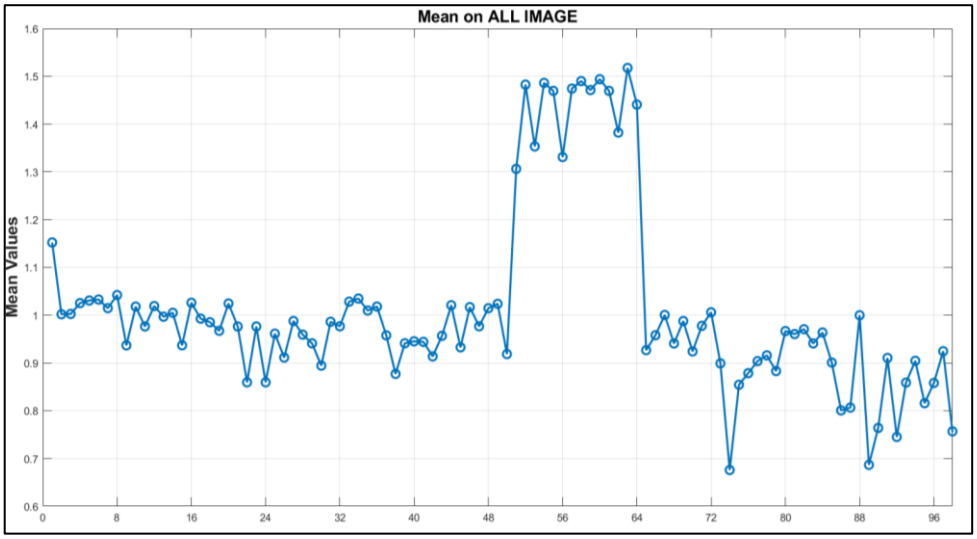

Figure 93: Results on All LEDs

The results showed in the previous pages do not follow a precise trend or pattern; what can be seen it is that with the Wednesday's samples the system has registered values a little bit over the other values. The system recorded values that were not in line with what was done during the other sampling days; these results, although they can be easily traced back to a human error in positioning the samples, can also be due to other different reasons; the turbidity levels corresponding to these peaks are quite low, as it is showed in the next section, explaining the peaks but another reason, discovered later, is that there was an anomaly in the wastewater plant tank where the samples were collected.

The other analysis conducted through the *MATLAB* toolboxes shown in the following pages are the results obtained with the 96 samples taken from Ilderton plant. A premise must be made, the data used were not sufficient to have a proper analysis, nevertheless the results gained are promising for a deeper analysis in the future when there will be time to get a bigger dataset to work with.

The results are showing the different models obtained through the *Classification Learner* use several classifiers: in the *figure 94* the model uses a *Fine KNN* which uses a nearest neighbor technique and has a good prediction accuracy with small dimensions. The number of neighbors is set to one, the distance is calculated as Euclidean, and the distance is not weighted.

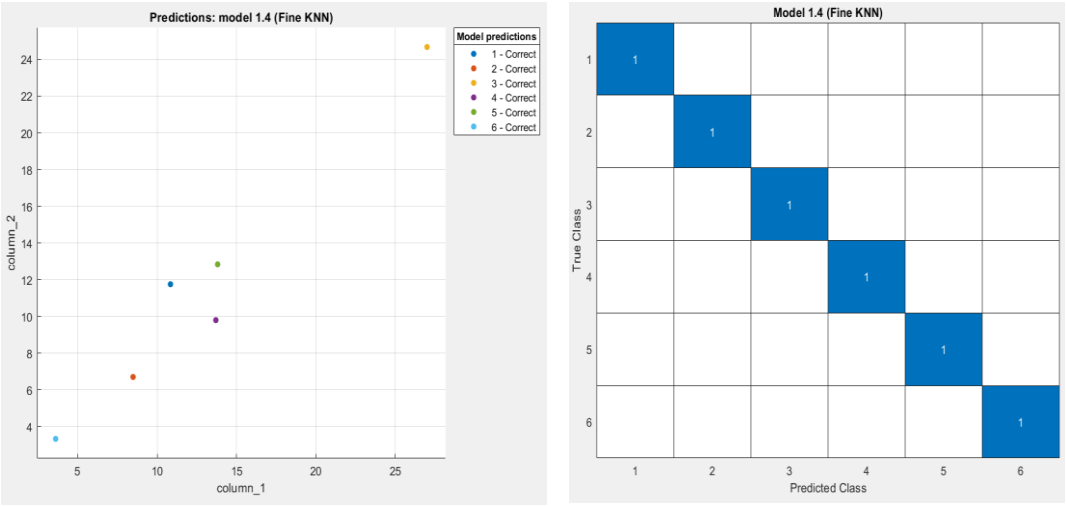

Figure 94: Results Fine KNN Model

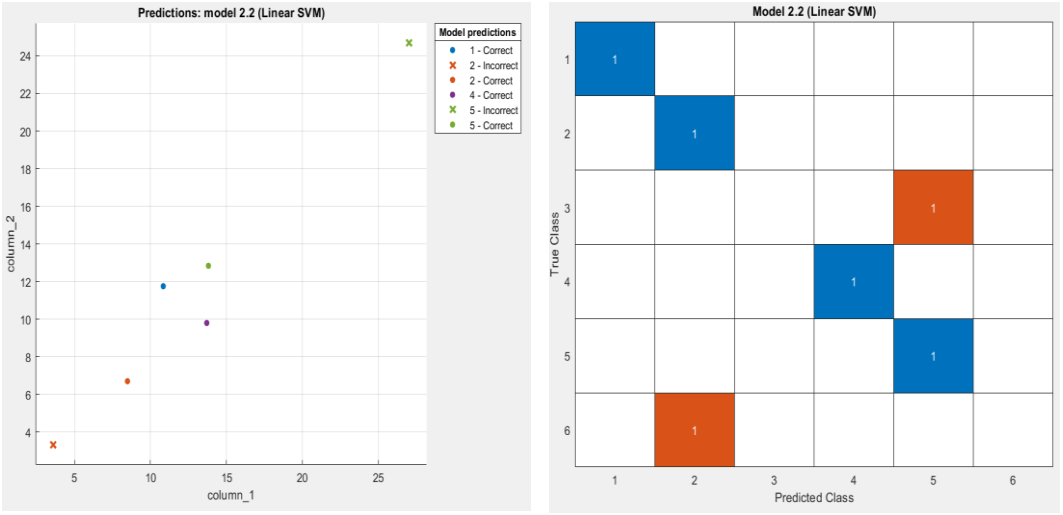

Figure 95: Results Linear SVM Model

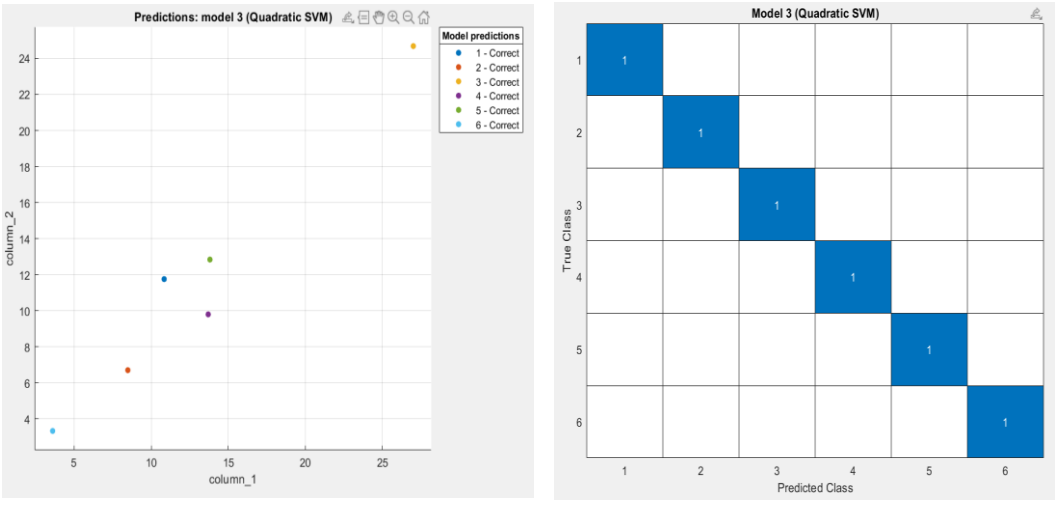

Figure 96: Results Quadratic SVM Model

In the *figures 95 and 96* are shown the results from two different technique, the linear SVM and the quadratic SVM. The first uses a simple linear separation between classes and the results are not the best in fact, the confusion matrix and the scatter plot show some prediction error by the model; the second instead, with a quadratic SVM, has shown better results over predictions.

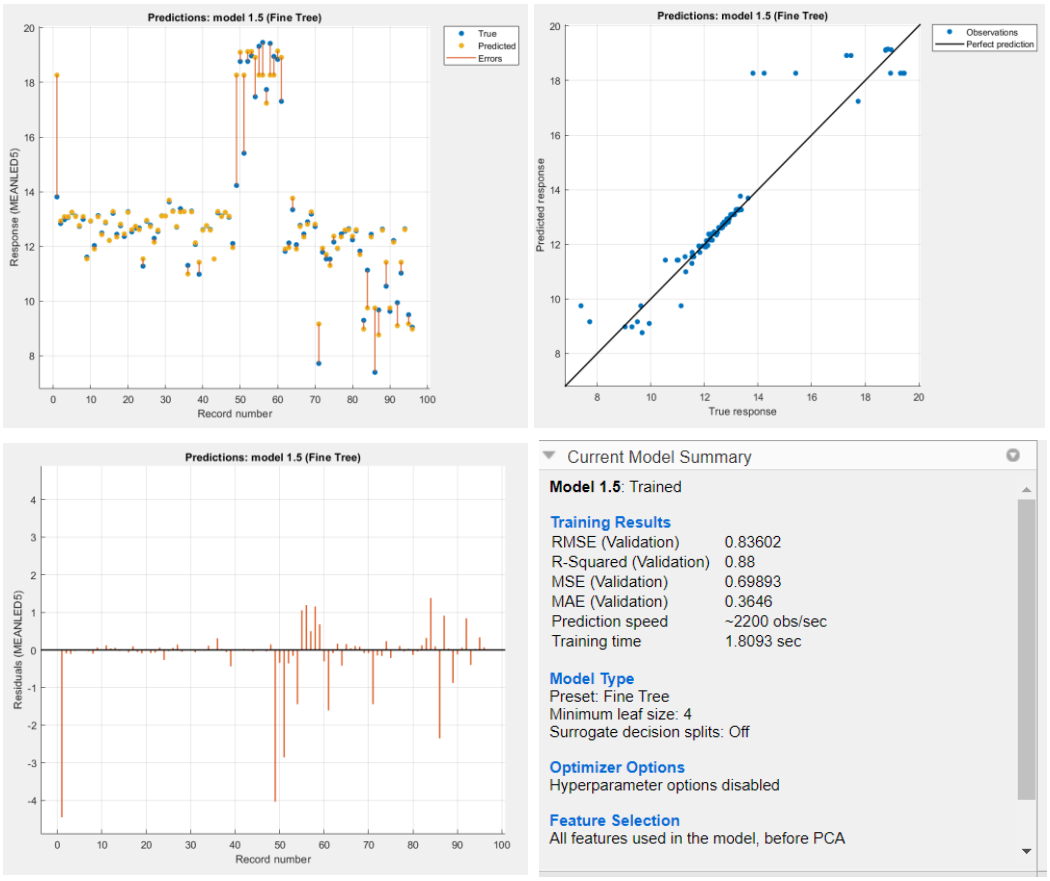

Figure 97: Results Fine Tree Model

About the Regression Learner app, the results shown in *figure 97* are about a Fine Tree Model; the model it has been chosen for its good results in predict the values with a very small error and a RMSE of 0,83602, a R-Squared value of 0,88 and for the fact that this method presents itself a high flexibility with many small leaves with a minimum size of four.

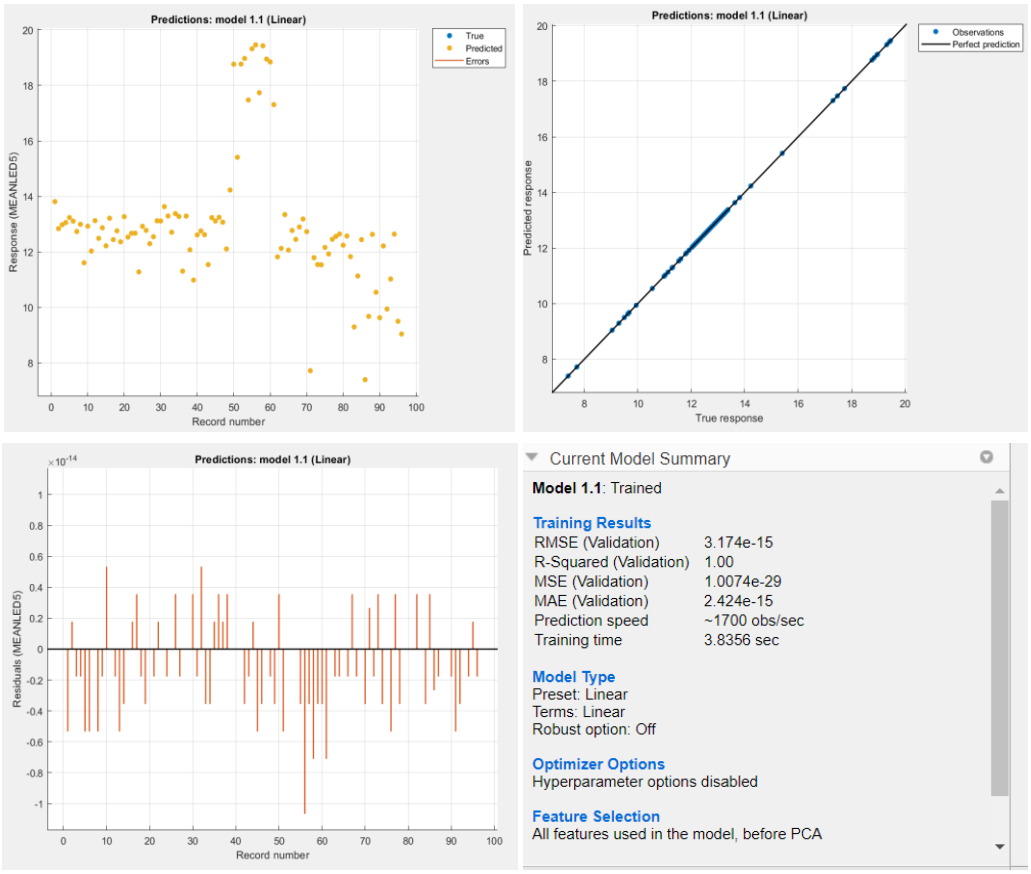

Figure 98: Results Linear Model

The other model presented in *figure 98* is a linear model, and even if this kind of model it uses linear predictors in the model parameters, it has a better fit with a RMSE of 3,174e^15 and a R-Squared of 1 as a prove of good validation.

What has been shown in the pages above is just a first analysis conducted on the samples taken over those four days. To obtain these results in both cases, for classification and regression models, have been validated using not a cross validation or an holdout validation but a resubstitution validation; this technique has no protection against overfitting and the apps use the data for both training and testing. This method has to be used because the data were insufficient to have a proper analysis using a more accurate validation; nevertheless, the results obtained are very promising even with very simple models.

4.3 Results Comparison

The results shown in the following images are results that have been normalized on a scale of 0 - 1 in order to be comparable on the same scales and to be read together, to understand the similarities and possible trends present in the collected data.

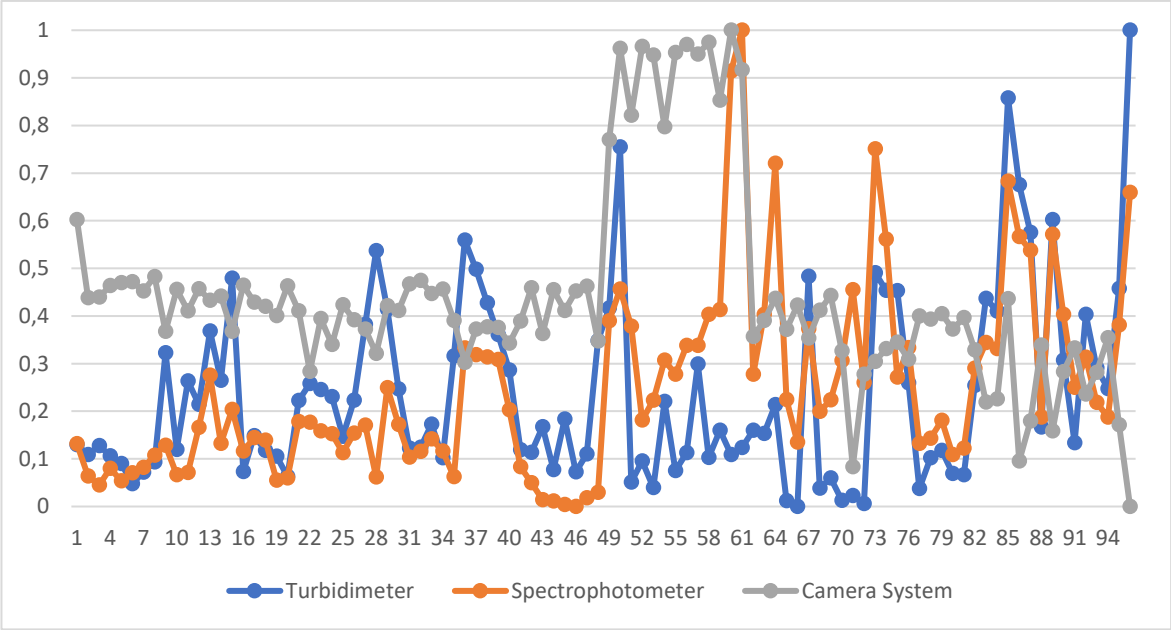

Figure 99: Normalized Data Comparison

The results that emerge from this first overlap immediately make us notice how the results obtained by the turbidimeter and the new system created are, as it should be, almost opposite.

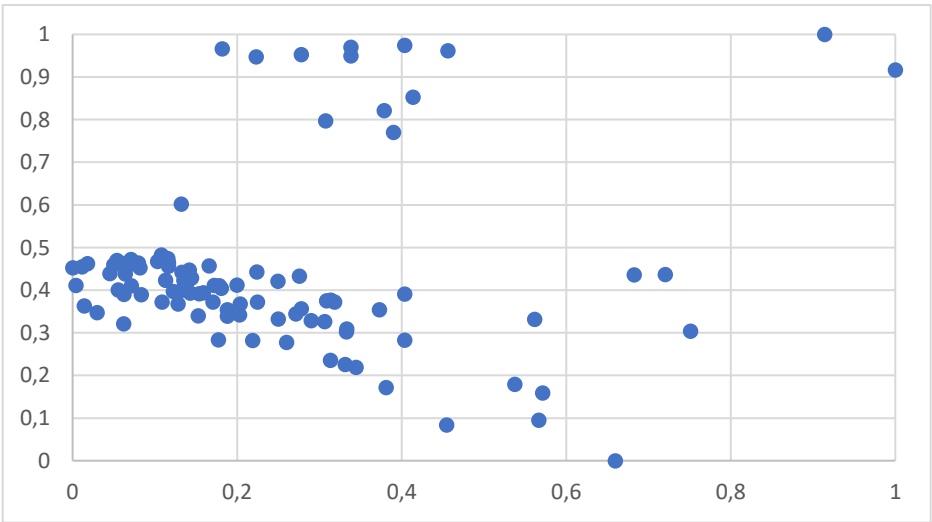

Figure 100: Correlation Between Absorbance and Pixels Mean Values

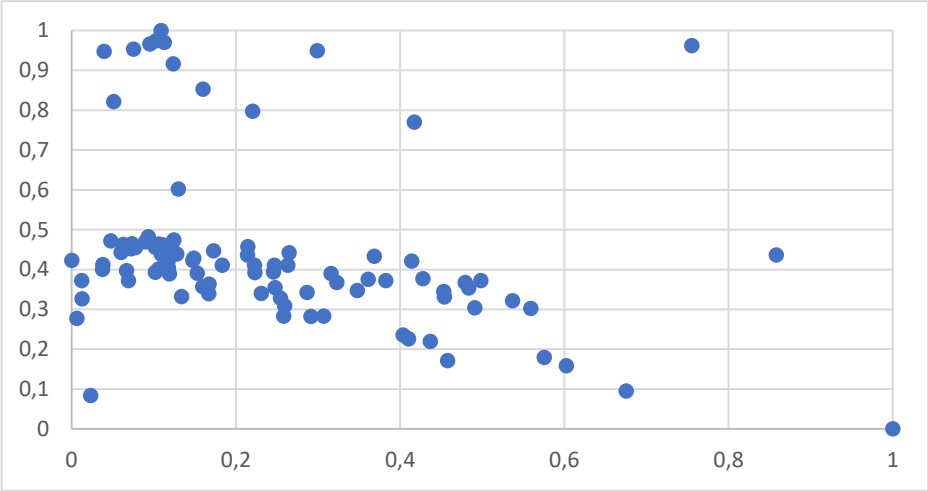

Figure 101: Correlation Between Turbidity and Pixels Mean Values

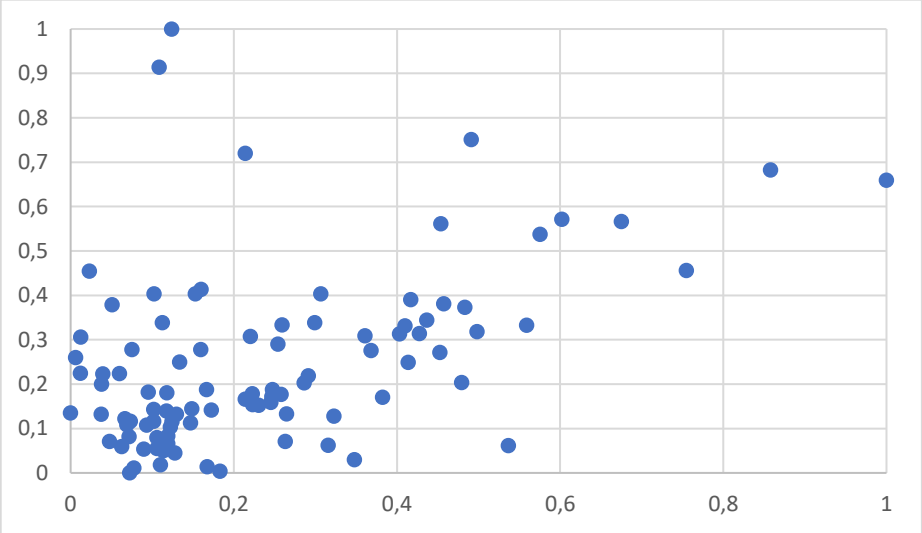

Figure 102: Correlation Between Absorbance and Turbidity Values

Over the scatterplots, that in this situation do not show neat trends or patterns the correlation factor between the sets of data has been calculated using the following formula:

$$Correl(X,Y) = \frac{\sum(x-\bar{x})(y-\bar{y})}{\sqrt{\sum(x-\bar{x})^2(y-\bar{y})^2}}$$

The results which are strictly related to the figures above are:

Data Considered	Correlation Factor
Turbidity & Pixels Mean Value	-0,33715
Absorbance & Pixels Mean Values	0,12078
Absorbance & Turbidity	0,4649

Table 7: Correlation Data

Even if the values calculated are not high and close to 1 or -1, they follow what was the expectation: the correlation between the turbidity and the mean values extracted from the camera's images is negative; this data confirm the fact that with a higher turbidity value the system reacts with a lower value of the pixels because the light rays are more attenuated by the water layer they have to go through. The other interesting value is the positive correlation between the absorbance values and the turbidity ones that can be explained as a consequence of more particles e sediments in the water samples bring to a higher value of absorbance of light rays.

To have another data to evaluate and consider, after a normalization of the data, each LED, with his precise wavelength, has been compared with the results of the absorbance taken by the spectrophotometer in that exact wavelength over the spectrum.

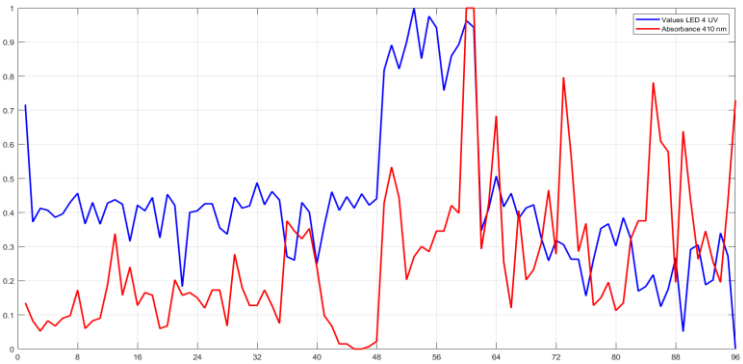

Figure 103: Comparing Absorbance Values at 410 nm and Results on LED 4 UV

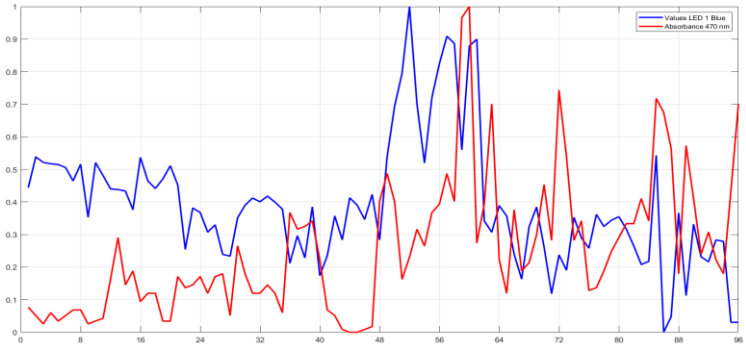

Figure 104: Comparing Absorbance Values at 470 nm and Results on LED 1 Blue

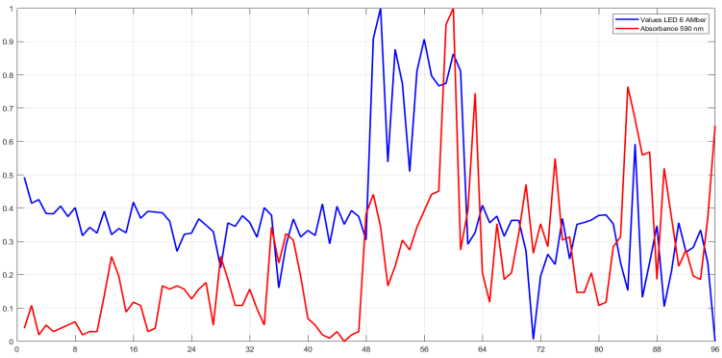

Figure 105: Comparing Absorbance Values at 590 nm and Results on LED 6 Amber

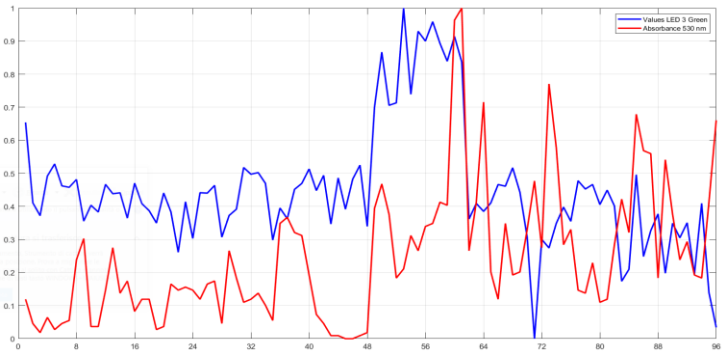

Figure 106: Comparing Absorbance Values at 530 nm and Results on LED 2 Green

4.3.1 Scattering Experiment Results

The results obtained from the experiments are showed in the following images, the pixels' mean values and the 3D surface generated from those values, to show the neat differences obtained.

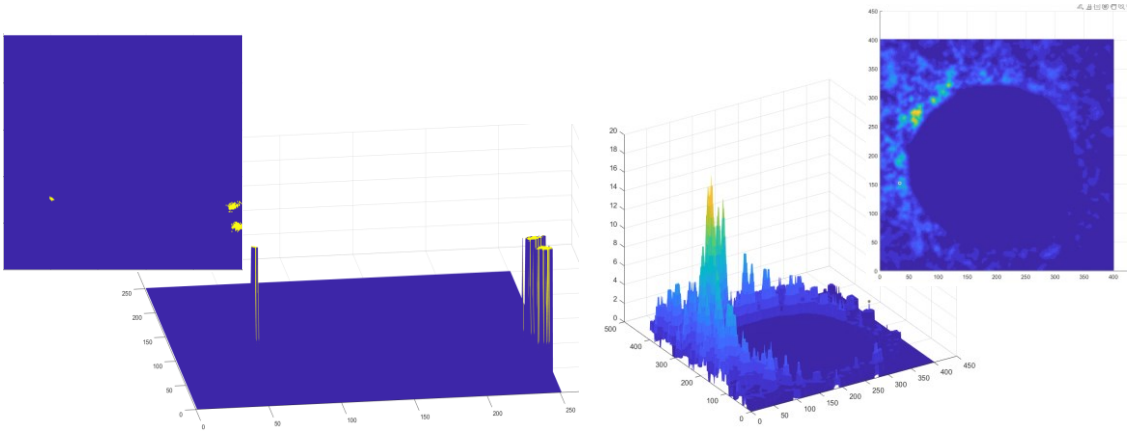

Figure 107: Plotting Results LED 5 Cold White Distilled Water Left and Friday Sample Right

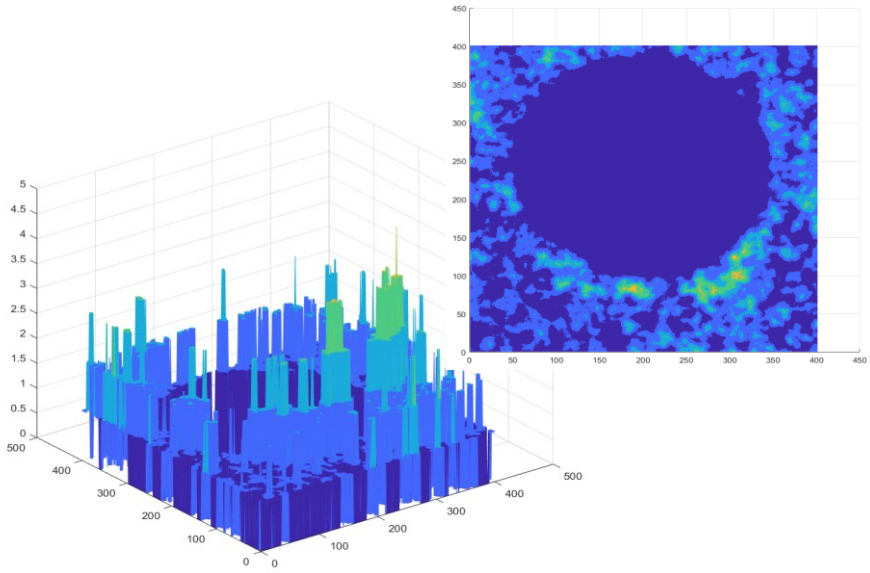

Figure 108: Plotting Results LED 4 UV Friday Sample

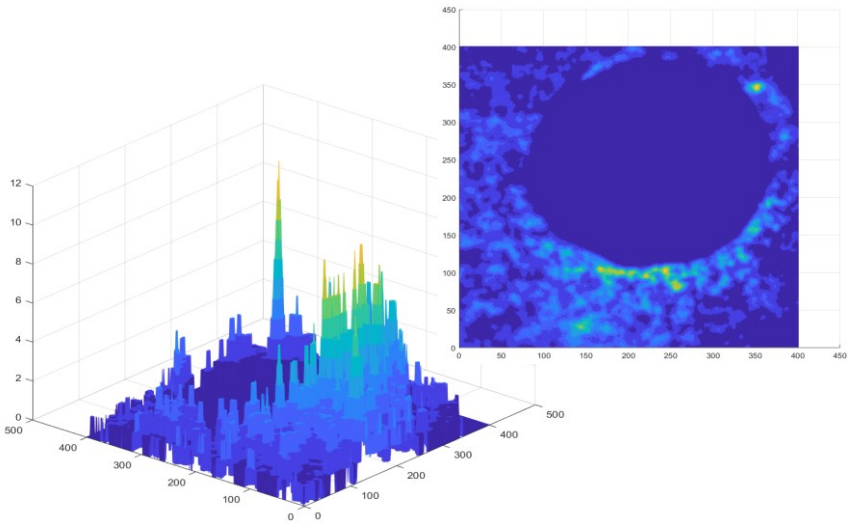

Figure 109: Plotting Results LED 2 Green Friday Sample

As it is showed in the figures above, as an example of the results obtained over the different LEDs, it is very clear the difference obtained with distilled water and a wastewater sample which present a higher turbidity and some particles in it that produce this phenomenon of scattering. Moreover, the mean values over each LED have been plotted too, confirming what it was already clear with the previous images.

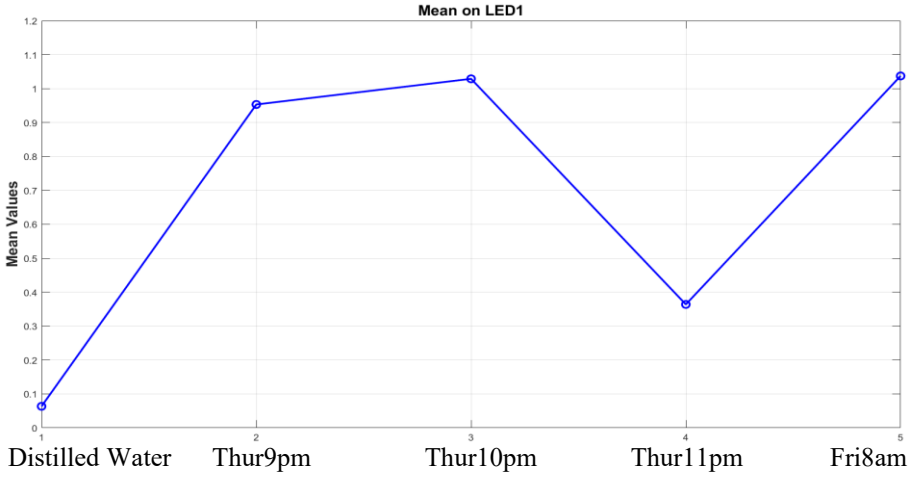

Figure 110: Pixels Mean Values on LED 1 Blue

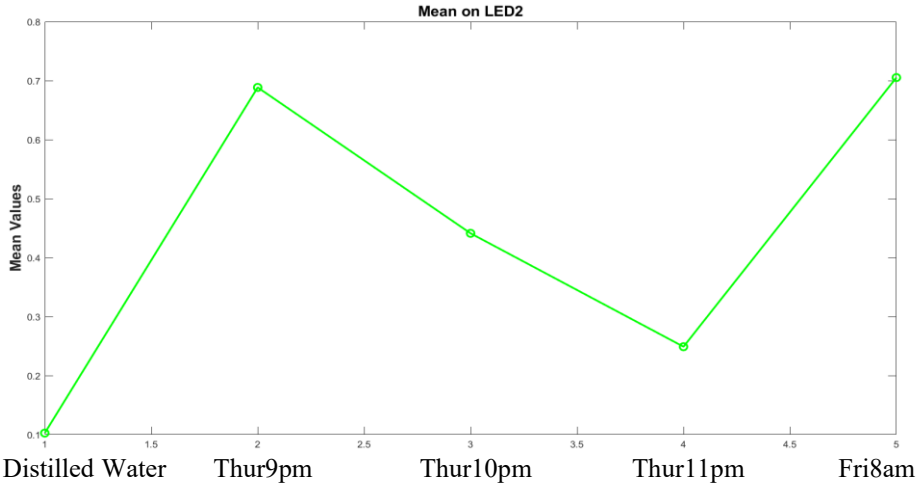

Figure 111: Pixels Mean Values on LED 2 Green

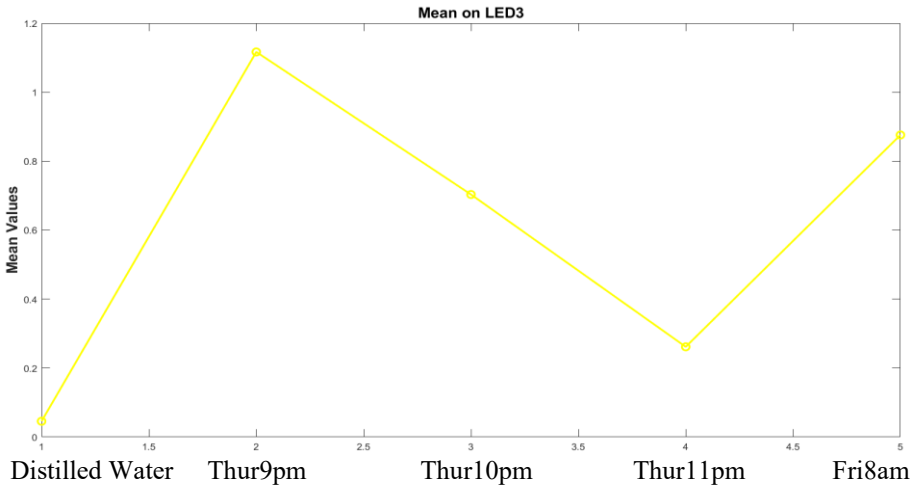

Figure 112: Pixels Mean Values on LED 3 Warm White

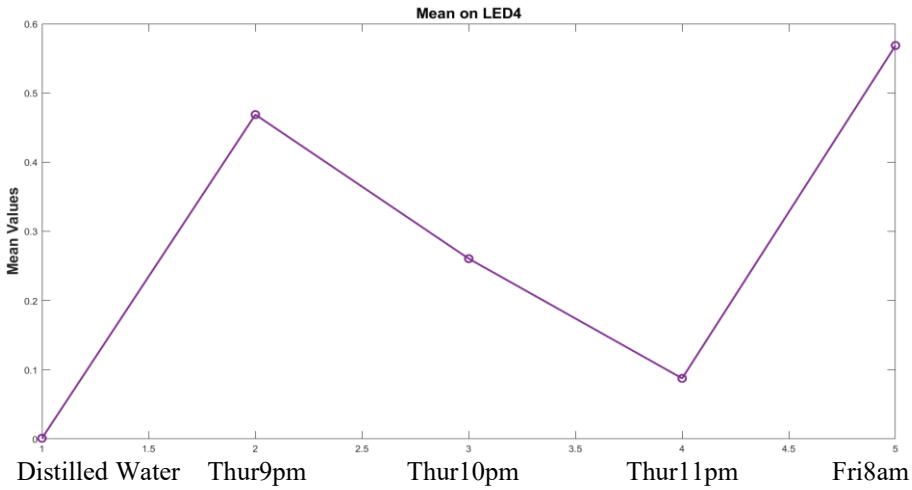

Figure 113: Pixels Mean Values on LED 4 UV

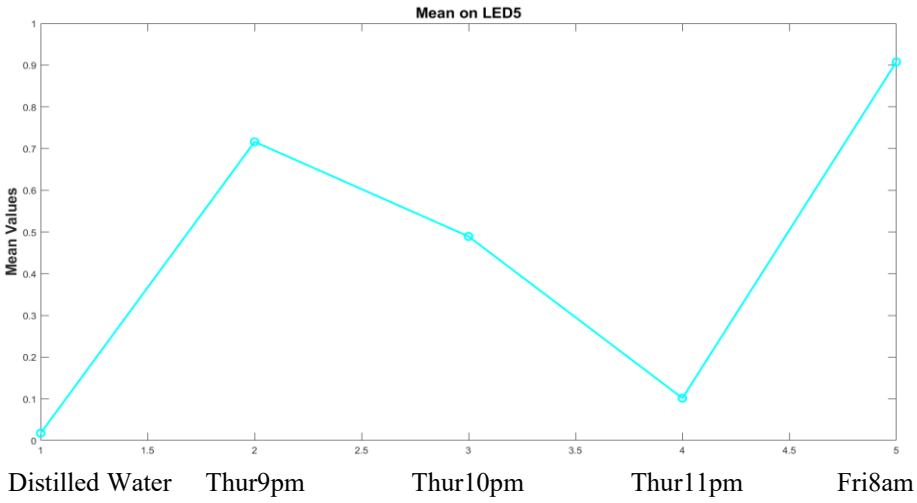

Figure 114: Pixels Mean Values on LED 5 Cold White

Data Considered	Correlation Factor
LED 1 Blue	0,892831
LED 2 Green	0,916958
LED 3 Warm White	0,869942
LED 4 UV	0,890518
LED 5 Cold White	0,875295

Table 8: Correlation Data

In this case too, the correlation factor between the values obtained and the results of the turbidimeter was calculated. Unlike previous experiments, where a negative correlation was expected and considered a good result, here a positive factor was expected; precisely the values obtained are not only positive but also very close to 1, indicating a close correlation between the values obtained from the chamber and turbidity.

Chapter 5: Conclusion and Future Development

In conclusion, through these experiments we wanted to understand if the basic idea was valid and could lead to significant results in the analysis of wastewaters.

The several tests, that have been conducted at first, have been necessary to understand how to calibrate and make the system work. As shown in the previous chapter, the results obtained are promising and validate the system created by Camera-LEDs through a direct comparison with some tools already present on the current market. Although the one used was a first prototype built following a trial-and-error heuristic method, the results presented bode well for the technology used.

The system is therefore presented as a technology that wants to be included in the control analysis of a wastewater plant, by making a simple check of the state of the wastewater coming out of a secondary stage of water treatment. In fact, the system does not aim to understand which pollutants were but to understand that there has been a variation from a previously evaluated steady state.

During the last week of work has been established, even if it is just a first prototype, how the model works detecting differences in various real wastewater samples during a period of time, simulating a real situation and comparing the results obtained with actual machines for water analysis.

The analysis carried out with the two different *MATLAB* toolboxes have been just the tip of the iceberg of what those analysis could bring and for sure with a bigger set of data, collected over a wider period of time will carry to better results in creating a precise and valid predicting model.

Hence, the validation of the idea tells us how we have just scratched the surface of what this system could be capable of doing, making us think of several other applications that the system can have, not only in the wastewater quality analysis but in other context too.

5.1 Next Steps

The next steps are going to be essential to develop a full working product; in this regard, various developments can be seen in the project that have not yet been realized due to a matter of time, but which will certainly be developed later.

The system created, as previously mentioned, is only a prototype to collect data in the laboratory; the next step would be, by reducing the size of the model, to create a second one that can be placed directly in a plant to monitor the trend of the data and by connecting it to an autosampler to give the signal to collect a sample whenever anomalous values are detected, to can be subsequently analyzed in the laboratory by other instruments. To do so the model would pass from a static one to a dynamic one with a waterflow that has to be flat and of a certain thickness; behind this research several calculous are going to be necessary to understand the pressure and speed of the waterflow.

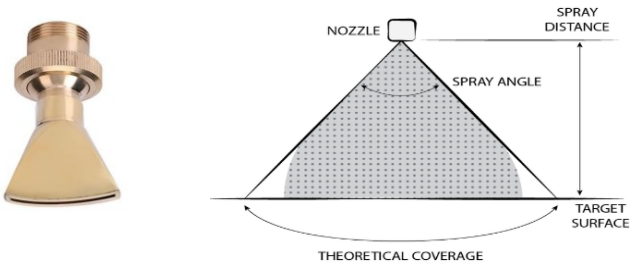

Figure 115: Flat Waterflow & Nozzle

Another step forward for the system would be to establish a wireless connection for transferring images in real time, from the camera to the laptop. To achieve this result several embedded solutions are available, such as a connection made via a *Raspberry o*r a more drastic solution would be the replacement of the camera itself, passing from a USB to a wireless camera. As said and showed previously the potential of this idea has been confirmed and at the same time it has been more than what could be expected. Hence, even if the realization of the project will not be easy or cheap, we firmly believe that it will still be worth carrying on to next level this project creating a new sensor in the wastewaters' scope.

Bibliography

- Chunyang He, Zhifeng Liu, Jianguo Wu, Xinhao Pan *2021* Future global urban water scarcity and potential solutions. Nature Communications
- Flannery Dolan, Jonathan Lamontagne, Robert Link *2021* Evaluating the economic impact of water scarcity in a changing world. Nature Communications.
- Environment and climate change Canada *2020* Municipal wastewater treatment Canadian environmental sustainability indicators.
- Safe Drinking Water Foundations *2021* Wastewater treatment.
- Safe Drinking Water Foundations *2021* Emerging contaminants
- L.S.Tam T.W.Tang G.N.Lau *2007* A pilot study for wastewater reclamation and reuse with MBR/RO and MF/RO systems. Desalination
- Archis Ambulkar 2016 Wastewater treatment. Britannica
- Gustavo A. S. Duarte, Helena D. M. Villela, Matheus Deocleciano *2020* Heat Waves Are a Major Threat to Turbid Coral Reefs in Brazil. Frontiers in Marine Science
- S.N. Patel, D. M. Patel, C. D. Patel, *2010* Self Emulsifying Drug Delivery System Journal of Global Pharma Technology
- Andrea G. Mann, Clarence C. Tam, Craig D. Higgins *2007* The association between drinking water turbidity and gastrointestinal illness: a systematic review. BMC Public Health
- R D Morris, E N Naumova, R Levin, R L Munasinghe *1996* Temporal variation in drinking water turbidity and diagnosed gastroenteritis in Milwaukee. Am. J Public Health
- Johan Pennekamp, R.J.C. Epskamp *1996* Turbidity caused by dredging; viewed in prospective. Terra et Aqua
- International Organization for Standardization *1999* Water quality: Determination of turbidity. International Standard ISO 7027
- European Commission *1998* Introduction to the new EU Water Framework Directive – Environment – European Commission. http://ec.europa.eu/environment/water/water-framework/info/intro_en.htm
- European Union *2014* European Union (Drinking Water) Regulations.
- American Public Health Association, American Water Works Association and Water Environment Federation *2012* Standard method 2130: Turbidity. In: Standard methods for the examination of water and wastewater. 22nd edition.
- ASTM International *2010* D6855-10: Standard test method for determination of turbidity below 5 NTU in static mode. ASTM International, West Conshohocken, Pennsylvania.
- ASTM International *2011* D7726-11: Standard guide for the use of various turbidimeter technologies for measurement of turbidity in water. ASTM International, West Conshohocken, Pennsylvania.

- Bertrand-Krajewski, J. L. *2004* TSS concentration in sewers estimated from turbidity measurements by means of linear regression accounting for uncertainties in both variables Water Sci. Technol
- Wu, J., Jiang, X. & Wheatley, A. *2009* Characterizing activated sludge process effluent by particle size distribution, respirometry and modelling. Desalination
- García-Mesa, J. J., Poyatos, J. M., Delgado-Ramos, F., Muñio,
- M. M., Osorio, F. & Hontoria, E. *2010* Water quality characterization in real biofilm wastewater treatment systems by particle size distribution. Bioresour. Technol
- Bersinger, T., Le Hécho, I., Bareille, G., Pigot, T. & Lecomte, A. *2015* Continuous monitoring of turbidity and conductivity in wastewater networks. Rev. des Sci. L'eau.
- Gitelson, A. A., Dall'Olmo, G., Moses, W., Rundquist, D. C., Barrow, T., Fisher, T. R., Gurlin, D. & Holz, J. *2008* A simple semi-analytical model for remote estimation of chlorophyll-a in turbid waters: validation. Remote Sens. Environ.
- Stedmon, C. A., Markager, S. & Bro, R. *2015* Tracing dissolved organic matter in aquatic environments using a new approach to fluorescence spectroscopy. Mar. Chem.
- Banna, M. H., Imran, S., Francisque, A., Najjaran, H., Sadiq, R., Rodriguez, M. & Hoorfar, M. *2014* Online drinking water quality monitoring: review on available and emerging technologies. Crit. Rev. Environ. Sci. Technol.
- Telesnicki, G. J. & Goldberg,W. M. *1995* Comparison of turbidity measurement by nephelometry and transmissometry and its relevance towater quality standards.
- Jouanneau, S., Recoules, L., Durand, M. J., Boukabache, A., Picot, V., Primault, Y., Lakel, A., Sengelin, M., Barillon, B. & Thouand, G. *2014* Methods for assessing biochemical oxygen demand (BOD): a review.Water Res.
- de Graaf, B. R., Williamson, F., Koerkamp, M. K., Verhoef, J. W., Wuestman, R., Bajema, B., Trietsch, E. & van Delft, W. *2012* Implementation of an innovative sensor technology for effective online water quality monitoring in the distribution network. Water Pract. Technol.
- Williamson, F., van den Broeke, J., Koster, T., Koerkamp, M. K. Verhoef, J.W., Hoogterp, J., Trietsch, E. & deGraaf, B. R. *2014* Online water quality monitoring in the distribution network. Water Pract. Technol
- Tomperi, J., Koivuranta, E., Kuokkanen, A., Juuso, E. & Leiviskä, K. *2016* a Real-time optical monitoring of the wastewater treatment process. Environ. Technol
- Tomperi, J., Koivuranta, E., Kuokkanen, A. & Leiviskä, K. *2016* b Modelling effluent quality based on a real-time optical monitoring of the wastewater treatment process. Environ. Technol.
- Joannis, C., Ruban, G., Gromaire, M. C., Bertrand-Krajewski, J. L. & Chebbo, G. *2008* Reproducibility and uncertainty of wastewater turbidity measurements. Water Sci. Technol
- Byung-Hyuk Kim, Jong-Eun Choi, Kichul Cho, Zion Kang, Rishiram Ramanan, Doo-Gyung Moon, and Hee-Sik Kim *2018* Influence of Water Depth on Microalgal Production, Biomass Harvest, and Energy Consumption in High-Rate Algal Pond Using Municipal Wastewater Journal of Microbiology and Biotechnology
- Hambly, A. C., Arvin, E., Pedersen, L. F., Pedersen, P. B., Seredyn´ska-Sobecka, B. & Stedmon, C. A. *2015* Characterising organic matter in recirculating aquaculture systems with fluorescence EEM spectroscopy. Water Res

- Logue, J. B., Stedmon, C. A., Kellerman, A. M., Nielsen, N. J., Andersson, A. F., Laudon, H., Lindström, E. S. & Kritzberg, E. S. *2016* Experimental insights into the importance of aquatic bacterial community composition to the degradation of dissolved organic matter. ISME J
- Melik, D. & Fogler, H. *1983* Turbidimetric determination of particle size distributions of colloidal systems. J. Colloid Interface Sci.
- Darragh Mullins, Derek Coburn, Louise Hannon, Edward Jones, Eoghan Clifford and Martin Glavin *2018* A novel image processing-based system for turbidity measurement in domestic and industrial wastewater. Water Science and Technology
- Hannon, L. *2016* An Investigation of Operational Test Practices at Wastewater Treatment Plants. National University of Ireland Galway

Ringraziamenti

Arrivati a conclusione di questo percorso vorrei spendere qualche riga per ringraziare chi mi ha aiutato a raggiungere questo risultato

Vorrei iniziare ringraziando il Professor Scaradozzi che in questi anni di esami, laboratori e tesi mi ha guidato attraverso i suoi preziosi consigli

Un grazie va alla mia famiglia, ai miei genitori per i loro immensi sacrifici, alla pazienza per avermi come figlio. Credo non abbiano ancora capito cosa realmente abbia studiato e quale enorme opportunità mi abbiano concesso ma sono sempre stati al mio fianco dandomi fiducia e appoggiando le mie scelte e ve ne sarò sempre grato

Grazie Marco per essere sempre il fratello che non merito ma di cui ho bisogno

Nonna Lia, l'unica che riesce a non farmi seguire la dieta senza rimpianti, nei nostri discorsi più di tutti mi hai insegnato a riflettere sulle scelte, sulle persone e sulla vita, grazie

Grazie Marco, Simone, Lorenzo, Matteo ci siete sempre e per me incarnate il vero significato della parola amicizia

Un grazie va anche ai dottorandi Carmine, Maddalena, Samuele e Michele che ho avuto la fortuna di conoscere e di poter definire amici, persone che reputo eccezionali dal punto di vista accademico e umano e che mi hanno insegnato tanto

Infine, vorrei fare un ringraziamento particolare al Professor Santoro per la preziosa opportunità. Si è rivelato capace di insegnarmi, di aiutarmi ma soprattutto sopportarmi, rivelandosi Il Professore che tutti sogniamo di avere.

Home is behind

The world ahead

And there are many paths to tread

Through shadow

To the edge of night

Until the stars are all alight…

Engineering Department

Master's Degree Course in Computer and Automation Engineering

Engineering Department

Master's Degree Course in Computer and Automation Engineering